

Performance analysis of carbon-doped titania counter electrode for dye sensitized solar cells



By

Faisal Abbas

Reg # 00000276310

Session 2018-20

Supervised by

Dr. Sehar Shakir

U.S. – Pakistan Center for Advanced Studies in Energy (USPCAS-E)

National University of Sciences and Technology (NUST)

H-12, Islamabad 44000, Pakistan

August 2022

Performance analysis of carbon-doped titania counter electrode for dye sensitized solar cells



By

Faisal Abbas

Reg # 00000276310

Session 2018-20

Supervised by

Dr. Sehar Shakir

**A Thesis Submitted to U.S.-Pakistan Center for Advanced Studies in
Energy partial fulfillment of the requirements for the degree of
MASTER of SCIENCE in
ENERGY SYSTEMS ENGINEERING**

U.S. – Pakistan Center for Advanced Studies in Energy (USPCAS-E)

National University of Sciences and Technology (NUST)

H-12, Islamabad 44000, Pakistan

August 2022

THESIS ACCEPTANCE CERTIFICATE

Certified that final copy of MS/MPhil thesis written by **Mr. Faisal Abbas** (Registration No. **00000276310**), of U.S.-Pakistan Center for Advanced Studies in Energy has been vetted by undersigned, found complete in all respects as per NUST Statues/Regulations, is within the similarity indices limit and is accepted as partial fulfillment for the award of MS/MPhil degree. It is further certified that necessary amendments as pointed out by GEC members of the scholar have also been incorporated in the said thesis.

Signature: _____

Name of Supervisor: Dr. Sehar Shakir

Date: _____

Signature (HoD): _____

Date: _____

Signature (Dean/Principal): _____

Date: _____

Certificate

This is to certify that work in this thesis has been carried out by **Mr. Faisal Abbas** and completed under my supervision in the Advanced Energy Material Lab laboratory, US-Pakistan Center for Advanced Studies in Energy (USPCAS-E), National University of Sciences and Technology, H-12, Islamabad, Pakistan.

Supervisor:

Dr. Sehar Shakir
USPCAS-E
NUST, Islamabad

GEC Member 1:

Dr. Nadia Shahzad
USPCAS-E
NUST, Islamabad

GEC Member 2:

Dr. Asif Hussain
Khoja
USPCAS-E
NUST, Islamabad

GEC Member 3:

Dr. Mustafa Anwar
USPCAS-E
NUST, Islamabad

HOD-ESE:

Dr. Rabia Liaquat
USPCAS-E
NUST, Islamabad

Dean/Principal:

Prof.Dr. Adeel Waqas
USPCAS-E
NUST, Islamabad

DEDICATION

I dedicated this thesis to my loving parents, respected teachers, and all my loyal friends, who encouraged and motivated me throughout this journey to accomplish this task.

Abstract

Fossil fuels play an important role in creating a balance between the energy supply and demand, but the use of fossil fuels is associated with the adverse climate change effect and rise in global temperature. To overcome these adverse effects, scientists are trying to shift toward renewable energy sources especially solar energy which has huge global potential. In this scenario, DSSC is a new and promising third-generation-based technique that has an edge over others due to its low cost, simple assembly procedure, environment-friendly nature, and good power conversion efficiencies. One of the most important components of DSSC that significantly affect the performance is the counter electrode, which acts as a catalyst and is responsible for the reduction of triiodide ions in the redox couple. In this study, Carbon-doped titania (C-TiO₂) CEs were fabricated by using the hydrothermal synthesis method. Four different weight ratios are used by varying the amount of glucose monohydrate 0.25g (5% of TiO₂), 0.5 g (10 % of TiO₂), 0.75 g (15 % of TiO₂), and 1g (20 % of TiO₂) against 5 g of anatase titania. Doctor blade coating was used to coat the paste onto the FTO glass substrate. By doping carbon into the titania, the cyclic voltammetry measurements showed the improved electrocatalytic activity towards the reduction of triiodide ions in the redox mediator to regenerate the dye molecules quickly, fast charge transfer rate, and low recombination rate in the redox mediator and in the oxidized dye molecules. Meanwhile, the optimized ratio 15C-TiO₂ CE in DSSC showed an excellent 1.56% photo conversion efficiency, quite close to platinum's 2.12% efficiency. By showing comparable electrocatalytic activity and photo conversion efficiency, low-cost C-TiO₂ CE (CE) is a promising substitute to replace the expensive platinum CE in the DSSC.

Keywords: *CE, carbon, titania, carbon doped titania, DSSC*

Table of Contents

Abstract	v
List of Figures	ix
List of Tables	x
List of Abbreviations	xi
List of Publications	xii
Chapter 1: Introduction	1
1.1 The Importance of Renewable Energy	1
1.2 Solar Cells	3
1.3 Photovoltaic Technology	4
1.3.1 Construction of a Solar Cell	5
1.3.2 Working Principle of Solar Cell	6
1.3.3 Photovoltaic Performance (I-V Characteristics)	6
1.4 Generations of Solar Cells	9
1.4.1 First Generation Solar Cells	9
1.4.2 Second Generation Solar Cells	10
1.4.3 Third Generation Solar Cells	11
1.4.3.1 Dye-Sensitized Solar Cell	12
1.5 Problem Statement	13
1.6 Research Objectives	14
1.7 Challenges in Research	14
1.8 Thesis Outlines	15
1.9 Scope of Thesis	16
Summary	17
References	18
2.1 Background of DSSC	21
2.2 Basic Structure of DSSC	21
2.2.2 Working Electrode / Photoanode	23
2.2.3 Dyes	23
2.2.4 Electrolytes	24
2.2.4.1 Liquid Electrolytes	25
2.2.4.2 Quasi-Solid State Electrolytes	25
2.2.4.3 Solid electrolytes	26
2.2.5 Counter Electrode	26

2.2.5.1 Counter Electrode materials for DSSCs.....	26
Summary.....	30
References	31
Chapter 3: An Introduction of Experimentation and Review of Characterization Techniques ...	36
3.1 Experimentation.....	36
3.1.1 Synthesis of carbon-doped titania powder material	36
3.1.2 Fabrication of CE.....	37
3.1.3 Fabrication of Photoanode	38
3.1.4 Fabrication of DSSC's	38
3.1.5 Characterization of CEs	38
3.2 Review of Synthesis Methods.....	39
3.2.1 Thermal Decomposition.....	39
3.2.2 Hydrothermal Method.....	40
3.2.3 Chemical vapor deposition.....	40
3.3 Review Techniques of Fabrication of DSSC	41
3.3.1 Doctor blade.....	41
3.3.2 Spin coating.....	42
3.3.3 Screen printing	43
3.4.1 X-ray diffraction	43
3.4.1.1 Working principle	44
3.4.2 Scanning electron microscope.....	44
3.4.2.1 Working principle	44
3.4.2.2 Sample preparation.....	45
3.4.3 Energy dispersive X-ray Spectroscopy	46
3.4.4 Raman Spectroscopy	46
3.4.4.1 Principle of Raman Spectroscopy	47
3.4.5 Cyclic Voltammetry.....	48
Summary.....	49
References	50
Chapter 4: Results and Discussion.....	52
4.1 Results and Discussion.....	52
4.1.1 X-Ray Diffraction	52
4.1.2 SEM/EDS.....	534
4.1.3 Raman Spectroscopy.....	55
4.1.4 Cyclic Voltammetry.....	556

4.1.5 I-V Characteristic Curve	57
Summary.....	60
References.....	61
Chapter 5: Conclusions and Future Recommendations	63
5.1 Conclusions.....	63
5.2 Future Recommendations	63

List of Figures

Figure1-1	Estimated Renewable Share of Total Final Energy Consumption (TFEC),2009&2019(IEA, 2021).....	2
Figure 1-2	Total Renewable Energy Share in 2019 according to (IEA, 2021)	3
Figure 1-3	Diagrams depicting Solar cell, Panel, Module and Array	4
Figure 1-4	Schematic representation of a solar cell with n and p type layers (ACS, 2022).....	5
Figure 1-5	I-V /PV Characteristic of a Solar Cell.....	8
Figure 1-6	Diagram depicting difference between mono and poly crystalline solar cells	9
Figure 1-7	Flexible and transparent thin films second generation based solar cells	10
Figure 1- 8	Application of building integrated dye-sensitized solar cells.....	12
Figure 1- 9	Diagram depicting flow of thesis	15
Figure 2-1	Basic structure / components of dye sensitized solar cell.....	22
Figure 2-2	Basic molecular structure of a) N3 dyes b) N719 dyes c) black dyes.....	24
Figure 3-1	Method to be followed for the fabrication of CE.....	36
Figure 3-2	Synthesis of carbon doped titania CE followed by calcination in the tube furnace.	37
Figure 3-3	Schematic diagram of hydrothermal synthesis method	40
Figure 3-4	Chemical vapor deposition of graphene on the surface of substrate	41
Figure 3-5	Modern spin coater for sophisticated coating	42
Figure 3-6	Interaction of the x-ray electromagnetic radiations with the crystalline material in XRD.....	43
Figure 3-7	Probe beam and measuring particle in SEM	44
Figure 3-8	Schematic flow for sample preparation for SEM films	45
Figure 3-9	Electron interaction with specimen during EDS	46
Figure 3-10	Laser interaction with the specimen and raman spectrum with intensity peaks	47
Figure 4-1	XRD patterns of pristine TiO ₂ and C-TiO ₂ powders respectively	52
Figure 4-2	SEM images and EDS spectra of a,a1,a2) 5% C-TiO ₂ , b,b1,b2) 10% C-TiO ₂ , c,c1,c2) 15% C-TiO ₂ and d,d1,d2)20% C-TiO ₂ at 10µm and 1µm respectively	54
Figure 4-3	Raman Spectroscopy of carbon doped titania CEs a) 5C-TiO ₂ , b) 10C-TiO ₂ , c) 15C-TiO ₂ , and d) 20C-TiO ₂ respectively	55
Figure 4-4	Cyclic voltammograms obtained at scan rate of 100mV/sec for C-TiO ₂ CEs and platinum respectively, in an electrolyte containing 500mM LiClO ₄ , 10mM I ₂ and 50mM LiI in acetonitrile solution	56
Figure 4-5	Photocurrent density-voltage characteristics curves of C-TiO ₂ and Pt CEs	57

List of Tables

Table 2-1 History of DSSC's based upon different CE materials	27
Table 4-1 Photovoltaic properties of the DSSCs using C-TiO ₂ and platinum as CEs	58

List of Abbreviations

TFEC Total final energy consumption

GHGs Greenhouse gas emissions

CE Counter electrode

DSSC Dye sensitized solar cell

ITO Indium doped tin oxide

FTO Fluorine doped tin oxide

CVD Chemical vapor deposition

XRD X-ray diffraction

SEM Scanning electron microscope

CV Cyclic voltammetry

C-TiO₂ Carbon-doped titania

PV Photovoltaic

CO₂ Carbon dioxide

List of Publications

Journal Paper: Faisal Abbas, Mustafa Anwar, Asif Hussain Khoja, Nadia Shahzad, Muhammad Tahir, Muniba Ayub, Sehar Shakir*, “Performance analysis of carbon-doped titania (C-TiO₂) counter electrode (CE) for dye sensitized solar cells (DSSCs)” Journal of Materials Science: Materials in electronics, **Status: Submitted**

Journal Paper: Muniba Ayub, Ahad Hussain Javed, Nadia Shahzad, Zuhair S. Khan, Sehar Shahkir, Faroha Liaqat, Ghulam Shabir, Faisal Abbas , Sana Mehmood, Muhammad Imran Comparative study of Ruthenium complexes with sensitizers in ZnO based dye sensitized solar cell Shahzad, Journal of Materials in Electronics , **Status: Submitted**

Journal Paper: Muhammad Tahir, Muhammad Abd-ur Rehman, Asif Hussain Khoja, Mustafa Anwar, Adil Mansoor, Faisal Abbas, Sehar Shakir “Praseodymium doped nickel oxide as hole-transport layer for efficient planar perovskite solar cells”, , Journal of alloys and compounds **Status: Submitted**

Acknowledgement

“Verily, there is ease after hardship”. First of all I want to thank my Allah Almighty for giving me patience and energy to accomplish this research work. I’m very thankful to my respected supervisor Dr. Sehar Shakir for encouraging and supporting me throughout the research. GEC members and especially lab engineer Dr. Asghar and Dr. Amir Satti helped me during experimentation and analysis. Thanks to Nisar Ahmad for guiding and helping me in interpretation of results. In this journey, my parents have been really a great source of motivation for me. It will be unfair not to mention my friends who were present there in my ups and downs and helped me with tackling uncertain conditions. I want to thank my fiends especially Zubair Ahmad, Hamza Sohail, Muhammad Kazim Murtaza, Muhammad Waqas Nazar, Muhammad Tahir and all other my loyal friends for their kind support to complete my thesis.

Chapter 1: Introduction

1.1 The Importance of Renewable Energy

Extensive use of fossil fuels is the main reason for increasing environmental concerns, due to GHGs emissions into the atmosphere. CO₂ has a major portion of GHGs and is the main reason for the climate change phenomenon and rise in average global temperature known as global warming. Global warming is not only a problem caused by combustion of the fossil fuels, other related problems like deforestation, acid precipitation, depletion of the ozone layer, deforestation, air pollution, and health problems associated with them[1]. Climate change has wide-ranging adverse impacts on the ecosystem, economy, health issues, and disturbance of the natural habitat. As fossil fuels are an exhaustible source of energy, one day they will be completely depleted depicting their consumption rate being more than the generation rate. As reported, about 80% of the primary energy needs to be fulfilled by using conventional fuels[2], and less than 15% of primary energy is provided by using renewable energy sources[3], this shows the world's energy dependency on the fossil fuels. Due to the rise in industrialization and population, it is estimated that energy demand will increase more than 300% than today at the end of the century[4]. To avert the global temperature rise by 2°C above the pre-industrial level, considerable efforts should be done, to decrease 25% CO₂ emissions by 2030, and reach carbon neutral by 2070, moreover to meet the ambitious target of the Paris agreement of avoiding 1.5°C, demands extensive effort to cut down the GHGs emissions level[5].

To mitigate the adverse effects of climate change and increase in global temperature, it is need time, to look for alternatives such as renewable energy sources to meet the supply and energy demands. Renewable energy sources are inexhaustible, reliable, and have the potential to replace fossil fuels shortly because they cause minute or no pollution and are environmentally friendly energy sources. Figure 1-1 compares the data of the total final energy consumption of renewable and fossil fuels energy sources share in 2009 and 2019, data proposed by the international energy agency[6]. It shows the TFEC consumption of fossil fuels almost remains changed from 80.2% in 2009 to 80.3% in 2019 respectively, while on the other hand, renewable TFEC shows an increment from 8.7% in 2009 to 11.2% in 2019 respectively. No doubt renewable energy share has been increased but the

rate to shift on renewables is still too low to meet the ambitious targets to cut down the emissions level to carbon neutral.

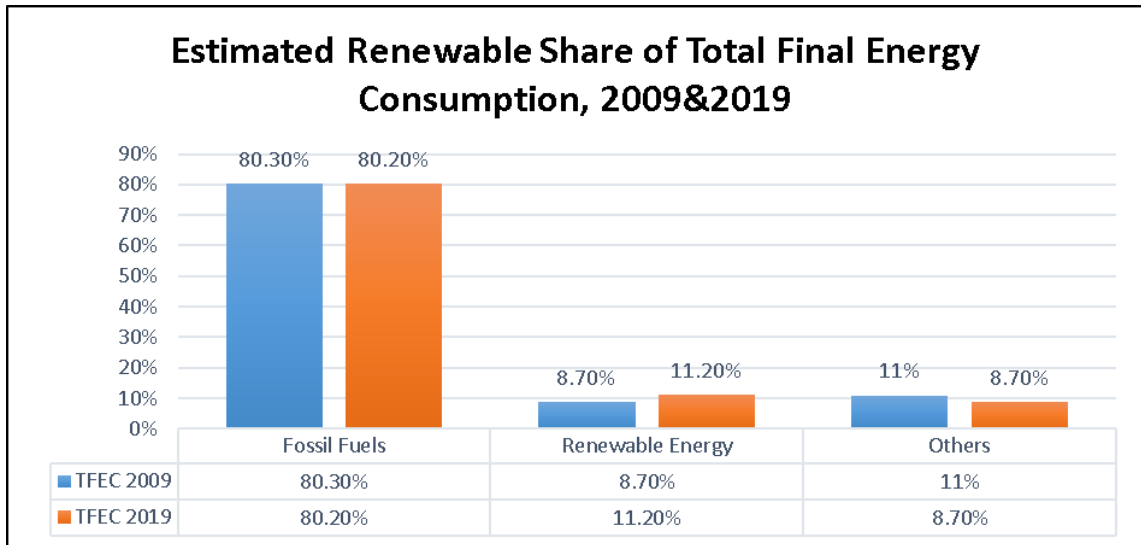


Figure 1-1 Estimated Renewable Share of Total Final Energy Consumption (TFEC), 2009&2019(IEA, 2021)

The reason behind the slow progress and adoption of renewable energy is due to the energy coming out from fossil fuels is cost-effective, infrastructure is readily developed, the huge capital investment required to build infrastructure for renewables, research continues to explore new fossil fuels reserves, and their invention, rise in energy demand due to increase in population, etc. These are the factors that impede the development of renewable energy sources and still have reliability on fossil fuels. Fossil fuels are a finite source of energy and they will run out eventually, according to a study[7], oil, gas, and coal will be completely depleted in 2052, 2060, and 2090 respectively.

In 2019 total renewable energy share in the TFEC is 11.2% which is almost more than 22% more than the consumption a decade ago. Figure 1-2 shows the renewable energy sources shares forming 1% by biofuels, 3.6% by hydropower, 4.2% by renewable sources of heat, and 2.4% by using renewable energy in power[6]. By keeping in COP26, the ambitious target has been set to increase the renewable energy share by more than 95% of today in the next five years by 2026[8]. To address the climate change issues and to meet the increasing energy demand, all renewable energy sources have potential and should be employed at an increasing rate for energy generation purposes. Among the renewable energy sources, solar energy is an effective alternative to fossil fuels, as it

carries out many benefits such as an abundance of sunlight, huge potential, free, green source, and no emissions[9].

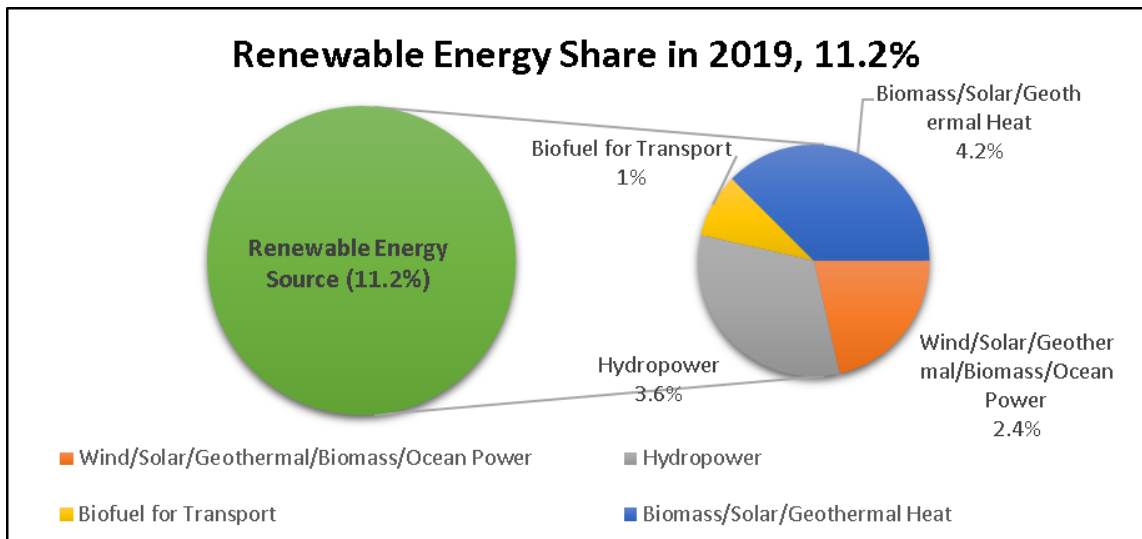


Figure 1-2 Total Renewable Energy Share in 2019 according to (IEA, 2021)

According to the World Bank, 93% of the global population lives where the solar potential lies between 3 KWh/KWp to 5 KWh/KWp[10]. By having huge potential, still, sun power only contributes 1.5% of the total world power generation[11]. Solar energy is a promising technology that has the potential to address climate change issues and will provide a free and green source of energy.

1.2 Solar Cell

A solar cell is a device that is used to convert solar light by selecting favorable wavelengths into electricity, mainly through the photovoltaic effect phenomenon described below. In 1905 Einstein published his paper regarding the photoelectric effect and got a noble prize in 1921. In 1914, layers of barriers were observed, later in 1954 at bell laboratories, Bell was an American scientist who developed the first silicon semiconductor-based solar cell, which absorbs the maximum sunlight to get enough electricity with 4% efficiency, later more work was done on this cell and achieved an efficiency about to 11%[12]. In 1976 at RCA laboratories David and Christopher develop the first amorphous silicon solar cell[13]. After these efforts regarding solar cell discovery, currently, solar energy is being investigated vigorously in form of different generation solar cells. Figure 1-3 depicts the photovoltaic cell, followed by the panel,

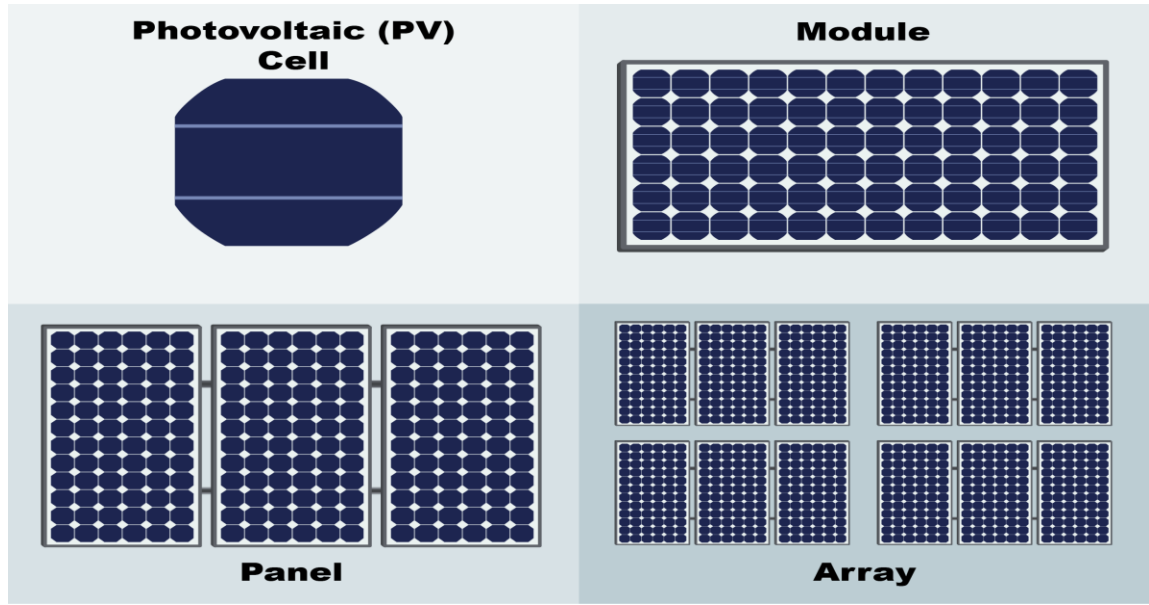


Figure 1-3 Diagrams depicting Solar cell, Panel, Module and Array

module, and solar array. A solar cell is a basic unit, by combining solar cells in a series, it takes a shape of a module, by combining modules it forms, and comes out as a panel, and by connecting panels, either in series or parallel way according to the requirements of power forms an array.

1.3 Photovoltaic Technology

Photovoltaic also known as PV technology defined as the process in which solar photons produce electricity (voltage) by using solar cells, while the solar cell is a device consisting of semiconductor materials such as silicon. Photon consists of energy packets that are present in the solar light and absorbed by the solar cells when they strike on the solar cells that are usually placed in series in form of a module. This phenomenon was first observed in 1954 by Bell Laboratories scientists, who developed a working silicon solar cell that generated an electric current when photons strike on the surface of the solar cell[14]. Solar energy has enormous potential and is being used in power plants ranging from small to large-scale systems to reduce the burden on the electricity grid and help out in using green energy to replace fossil fuels.

1.3.1 Construction of a Solar Cell

A solar cell consists of semiconductor materials with two layers called n-type and p-type layers, as well as having a depletion region depending upon the material used in the construction of SC as shown in Figure 1-4[15]. Silicon material has four electrons in its valence bond, so the p-type layer is made by doping an atom that has one less electron as

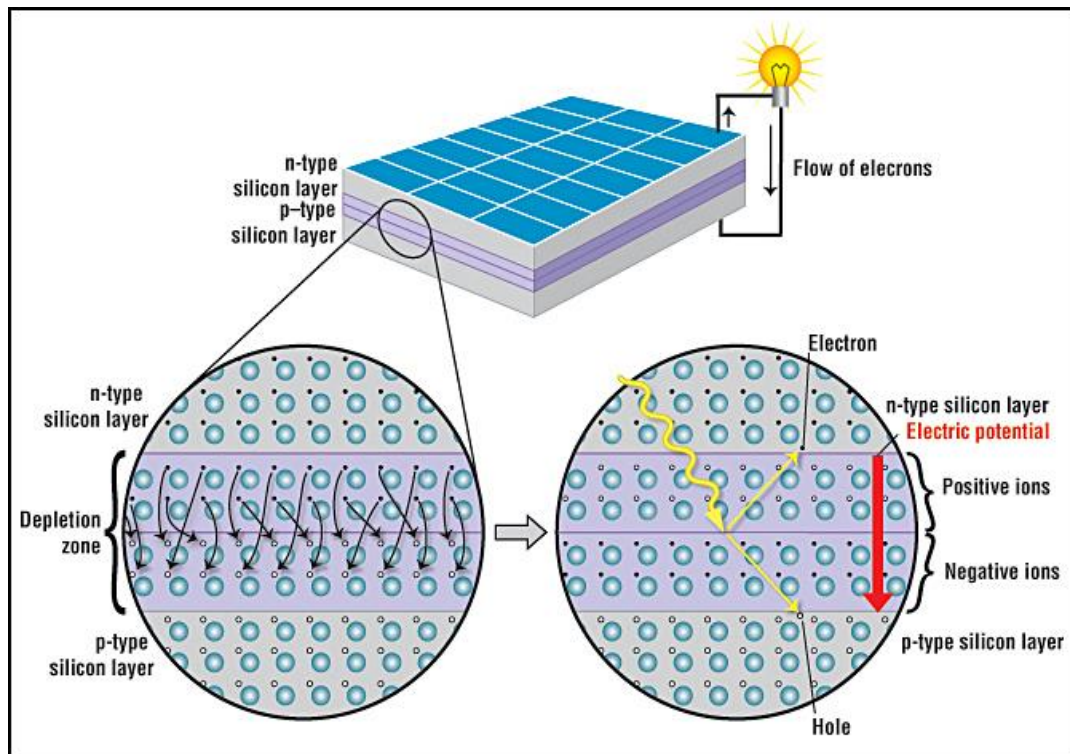


Figure 1-4 Schematic representation of a solar cell with n and p type layers (ACS, 2022)

compared to silicon in its out shell. Such as doping of aluminum, indium, or gallium is being done to form a p-type semiconductor material, dopant materials are also called trivalent impurities as they have three electrons in their valence band. In that way, a hole is created in the semiconductor material by adding trivalent atom impurity. P-type material has holes as they are in majority that's why they are also called majority charge carriers. Likewise, the n-type semiconductor material layer is formed by doping of an atom that has one more electron as compared to silicon material, in that way all the valence band vacancies are filled up by doping material, and an excess of the electron is present over there. Dopant materials to form n-type layers are arsenic or phosphorous etc. are also called pentavalent doping materials. The N-type layer is heavily doped and thin as compared to the p-type layer which is lightly doped and thick, to make sure the maximum

penetration of sunlight into the depletion region and maximum supply of electrons to a connecting load. In that way, both p-type positively charged and n-type negatively charged layers of a solar cell are produced. When p-type and n-type are connected to form a solar cell, then due to the imbalance of charge in both layers, the electrons in the n-type migrate toward the p-type layer, followed by the p-type holes that also migrate towards the n-type layer that are very close to each other, by combining of the electrons and holes form an internal field, called the depletion or depletion region, that further restricts the movement of electrons to pass through it until the energy more than depletion region field is provided to the solar cell to break this potential. This is the overall structure and formation of a solar cell.

1.3.2 Working Principle of Solar Cell

When a solar cell is placed in the ambient environment in the presence of sunlight, then photon of sunlight (energy packets) gives energy to the solar cell to produce an electric current. Overall solar cell working comprises three main steps,

- Absorption of sunlight
- Charge separation
- Conduction or charge collection

First solar light is absorbed in the visible range of 400nm-700nm wavelength by the surface of a solar cell, which comes through the glass. Cell absorbs the visible spectra and the energy required to break the depletion region is provided to get enough energy for conduction. In that way, all the holes and electrons go towards their sides, holes moves towards the p side while electrons move towards the n side, and charges are separated. Now, the solar cell has developed potential difference and if it is connected to a load, it enlightens the load and in that conduction takes place. Electrons move from n to the p-side where electrons meet with the holes and this cycle of conduction continues until enough energy photons are being received by the solar cells to break the junction barrier.

1.3.3 Photovoltaic Performance (I-V Characteristics)

I-V characteristics of a solar are determined by the IV curve which is a graphical representation between the voltage and current during exposure to sunlight. On the x-axis voltage values are present, while on the y-axis current is plotted. I-V curve is a tool for

determining the current, voltage, efficiency, and performance of the solar cell. It also tells about the power output under different conditions[16]. All the characteristics of a solar cell can be clearly shown in Figure 1-5. I-V characteristics are mainly dependent upon two factors, i) temperature, ii) radiations, both of the parameters affect the performance and have a direct impact on the solar efficiency and other parameters. Multiple parameters are associated with the I-V curve and are the following[17],

Short Circuit Current:

Current at which both of the output wires are connected when voltage is zero, in this condition solar cell gives highest value of current which is higher than normal current during operation. It is denoted by I_{sc} .

Maximum Current:

It is the normal current that solar cell provides during the nominal condition. It is represented by I_{mp} .

Voltage Open circuit:

Condition at which wires of the solar cell are not connected to any load when the current value is zero, solar cell provides the highest value of the voltage. It is denoted by V_{oc} .

Maximum Voltage:

Voltage of a solar cell during normal operation is represented by V_{mp} .

Maximum Power Point:

Power is the multiplication of voltage and current and it is the point in I-V curve when the multiple of current and voltage gives the maxim power value. It is denoted by M_{pp} . It is calculated by

$$M_{pp} = I_{mp} * V_{mp}$$

Fill Factor:

It is defined as the ratio of the maximum power to the theoretical power of the solar cell. It gives an idea about the quality and closeness of solar cells to unity. Normally, fill factor values are 0.7 to 0.8. It is represented by FF and calculated by the following formula

$$FF = \frac{V_{mp} * I_{mp}}{V_{oc} * I_{sc}}$$

Efficiency:

The efficiency of a solar cell determines the output power in a given scenario. It provides information about the overall performance. The efficiency of a solar is measured at standard conditions such as

Temperature: 25 °C

Irradiance: 1000 W/m²

Air mass: 1.5

Under these conditions, efficiency is determined by addressing all the ongoing phenomena inside the cell.

$$\eta (\%) = \frac{P_{max}}{1000 * Area} * 100$$

$$\eta(\%) = \frac{V_{oc} * I_{sc} * FF}{1000 * Area} * 100$$

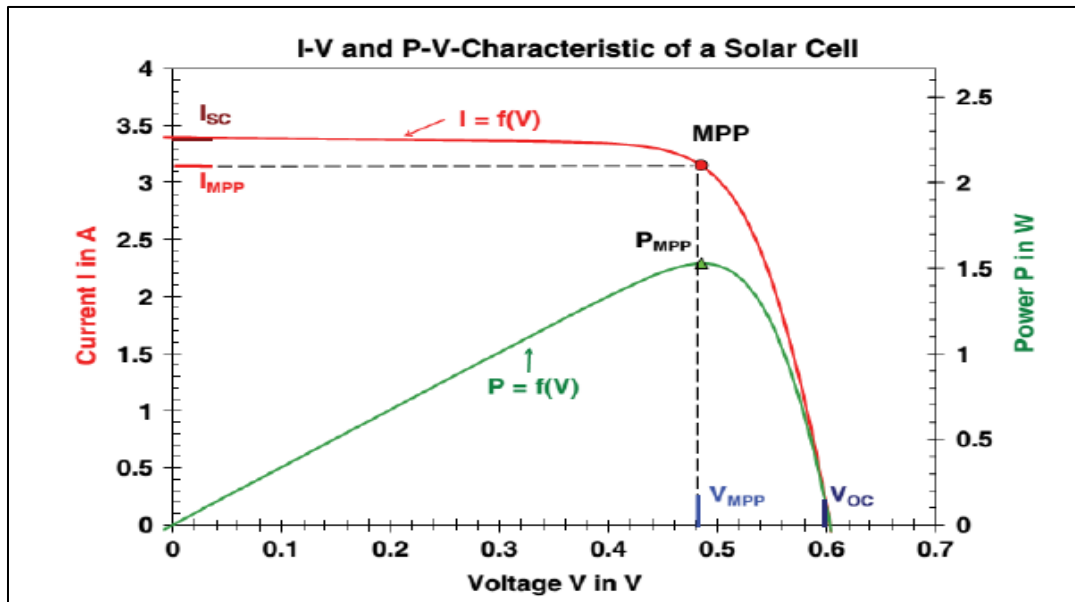


Figure 1-5 I-V /PV Characteristic of a Solar Cell

1.4 Generations of Solar Cells

Solar cells are divided into three generations depending upon the type of material used, working principle, and their maturity to be available at the commercial level.

- First Generation Solar Cells
- Second Generation Solar Cells
- Third Generation Solar Cells

1.4.1 First Generation Solar Cells

The first ever oldest cell fabricated was a silicon-based solar cell and lies in the first generation of solar cells. First generation solar cells are fabricated from silicon wafers. This is the highest efficient generation of solar cells as compared to other generations, but on the other hand, are very expensive because a method to fabricate them is an energy-intensive process called czochralski growth process. Mainly they are categorized into two major types based on the level of crystallization or the grain boundaries such as

- Poly Crystalline Solar Cells
- Mono Crystalline Solar Cells

Monocrystalline



Polycrystalline



Figure 1-6 Diagram depicting difference between mono and poly crystalline solar cells

Poly crystalline solar cells consist of multi crystals or are made of multi-grain boundaries which makes the poly solar cells impure, grain boundaries are visible on the surface of solar cells. While mono crystalline solar cells are the cells that are single crystal and are made through the controlled condition parameters from a poly crystal of silicon wafers. Another physical differentiation between them is mono cells are usually dark in color and they have an octagonal structure while poly cells have a dark blue color and are square in shape, as it can be clearly shown in Figure 1-6. Mono solar cells have good efficiency as compared to polycrystalline solar cells and surrounded less space as compared to poly cells as well as for aesthetic purposes, usually used. As mono cells are fabricated through a controlled environment that is a very complex part, that's why they are more costly than multi-crystal cells. Single crystal cell efficiency decreases as temperature rise more than 25 °C, due to these two issues, multi-crystal solar cells are the main competitor of mono cells, as they are easy to fabricate, have less energy requires, and are cost-effective. Although by carrying out research and modification in the fabrication of these cells, costs have been reduced considerably as compared to previous costs, still they are the most expensive generation solar cells and have overcome the solar market because of their high efficiency as compared to other generations.

1.4.2 Second Generation Solar Cells

Due to the energy-intensive and high cost of first-generation solar cells, scientists developed solar cells that were thin ranging between nanometers to a few micrometers,



Figure 1-7 Flexible and transparent thin films second generation based solar cells

while silicon-based solar cells were thick and quite high in weight. As their thickness is very low, that's why they are also called thin film solar cells. Amorphous silicon, cadmium telluride (CdTe), and copper indium gallium selenide ($\text{CuIn}_x\text{Ga}_{1-x}\text{Se}_2$, CIGS), gallium arsenide (GaAs) are the commonly known materials lies in this generation. Among all these photovoltaic materials, CIGS has shown the maximum cell efficiency reported 20%, but to make it at the commercial level at affordable prices is quite complex and difficult due to the rarity of indium material and tellurium. They are flexible and photovoltaic layers can be deposited onto a flexible substrate such as glass, plastic or metal, etc. Figure 1-7 shows the transparent and flexible thin film cells. Due to the use of less material, very thin layer size, and simple manufacturing techniques, make this type of generation of solar cells is cost-effective and an effective alternative to the previous one. They have large areas of application such as in calculators, cars, watches, and bags as well as can be deposited on windows for power generation and aesthetic purposes. Due to their flexibility, they face less drag or frictional forces as well as lower weight which makes them suitable for power applications. They include inorganic photovoltaic materials, which are hazardous to the environment and create multiple issues. Though they are cost-effective, they have less efficiency than first-generation solar cells as well as difficult to produce at a large scale due to the rarity of materials used.

1.4.3 Third Generation Solar Cells

Due to the rarity of materials, complex energy-intensive methods, and other cost-related issues in the abovementioned solar cells, this generation is based upon the cells that are being expected to get cost-effective and highly efficient photovoltaic devices. Still, this generation is in the laboratory phase, it will take time to commercialize after addressing all the issues such as they have lower efficiency, stability issues, degradation problems, etc. This generation consists of different cells based upon the material used such as

- DSSCs
- Quantum dot sensitized Solar Cells
- Perovskite Solar Cells
- Organic Solar Cells

Both DSSC and QDSC consist of organic materials in their formation which is big development toward replacing the first and second-generation inorganic solar cells. The highest DSSC reported efficiency is 14%, while QDSC has in the range of 8-10%. While OSC and Perovskite solar cells have 10-15% and 20% efficiencies respectively[18]. R&D is still going on to work on the parameters that hinder the performance of solar cells and trying to develop a solar cell that contains high efficiency and cost-effective and should be stable in the ambient environment with long span of life, so that they may come into the market at commercial level as they are environmentally friendly materials unlike of previous generations.

1.4.3.1 Dye-Sensitized Solar Cell

DSSC also known as Gratzel cell, is an emerging technology belonging to third-generation based solar cells and is under extensive research by scientists because this technology has multiple benefits over semiconductor-based cells. It was first developed in 1991 by O'Regan and Gratzel having an efficiency of 7% [19] only. By keeping in mind the benefits of this technology, extensive research is in the right direction, after three decades researchers have achieved an efficiency of almost 14% [20]. Usually, it consists of three major components, dye-sensitized mesoporous TiO_2 working electrode (WE) as photoanode, electrolyte, and pt CE as a cathode. Dye molecules absorb sunlight (photon) for the generation of electrons, excited electrons are injected into the conduction band of the semiconductor TiO_2 . The redox mediator is responsible for the regeneration of oxidized dye molecules. The CE is a key component to collect all the electrons through



Figure 1-8 Application of building integrated dye-sensitized solar cells

the external circuit via conducting substrate. The CE is also responsible for the regeneration of the redox mediator. Generally, platinum CE is used in DSSC applications, due to the superior electrocatalytic activity, stability and regeneration of the redox mediator with countless cycles in DSSC. However, cost and availability issues of Pt metal prevent the large-scale manufacturing of CEs in DSSC. Due to the high cost of Pt metal CE, various other low-cost materials have been used as CEs to get higher electrocatalytic activity, stability, and efficiency. The application of DSSC in building integrated windows can be clearly shown in Figure 1-8[21].

Though this efficiency is not highly efficient as compared to p-n junction technology, it is expected that this is a promising technology and an effective alternative that will be commercially adopted when all the issues such as stability issues, degradation of dye, and others issues will be addressed.

1.5 Problem Statement

CE in DSSC plays an important role in the charge transfer and the reduction of triiodide ions present in the redox mediator. Mostly, Pt CE is used in DSSC applications, because of its high activity, stability, and regeneration of the redox mediator with countless cycles in DSSC[19]. Cost and availability problems of Pt metal prevent the large-scale manufacturing of CE in DSSC. Due to the high cost of Pt metal CE, various other low-cost materials have been used as CEs for higher electrocatalytic activity, stability, and efficiencies such as carbon-based materials and others, such as graphene/carbon nanotubes[22], multiwall carbon nanotubes[23], hybrid carbon nanostructured[24], the conductive polymer[25], carbon nitride [26], nickel nitride [27], etc. Although the abovementioned CE alternative materials have good properties, still carbonaceous materials have an edge over them due to the following properties such as large surface area, good corrosion resistance, high conductivity, reactivity towards triiodide reduction as well as cost-effective and abundantly present[28]. Titanium dioxide (TiO_2) is also stable, non-toxic, and has good electric properties[29], so that's why cost-effective C- TiO_2 material CEs been used in my research to replace expensive Pt CE.

1.6 Research Objectives

DSSC is an evolving and promising technology for future solar cells and the intended objective of my research are the followings,

- To synthesize low-cost and efficient C-TiO₂ CE for DSSCs.
- To study the structural, morphological, and electrochemical characteristics of the CE
- To study the electrical properties of the fabricated CE

1.7 Challenges in Research

Addressing the following challenges in DSSC can pave the way toward commercialization.

- Incomplete dye regeneration due to sluggish kinetics of CE.
- As dye degrades under ambient conditions, the power conversion efficiency of the cell decreases
- Reliability and stability problems

1.8 Thesis Outline

The flow diagram depicts all the chapters that have been discussed in detail throughout the thesis in Figure 1-9.

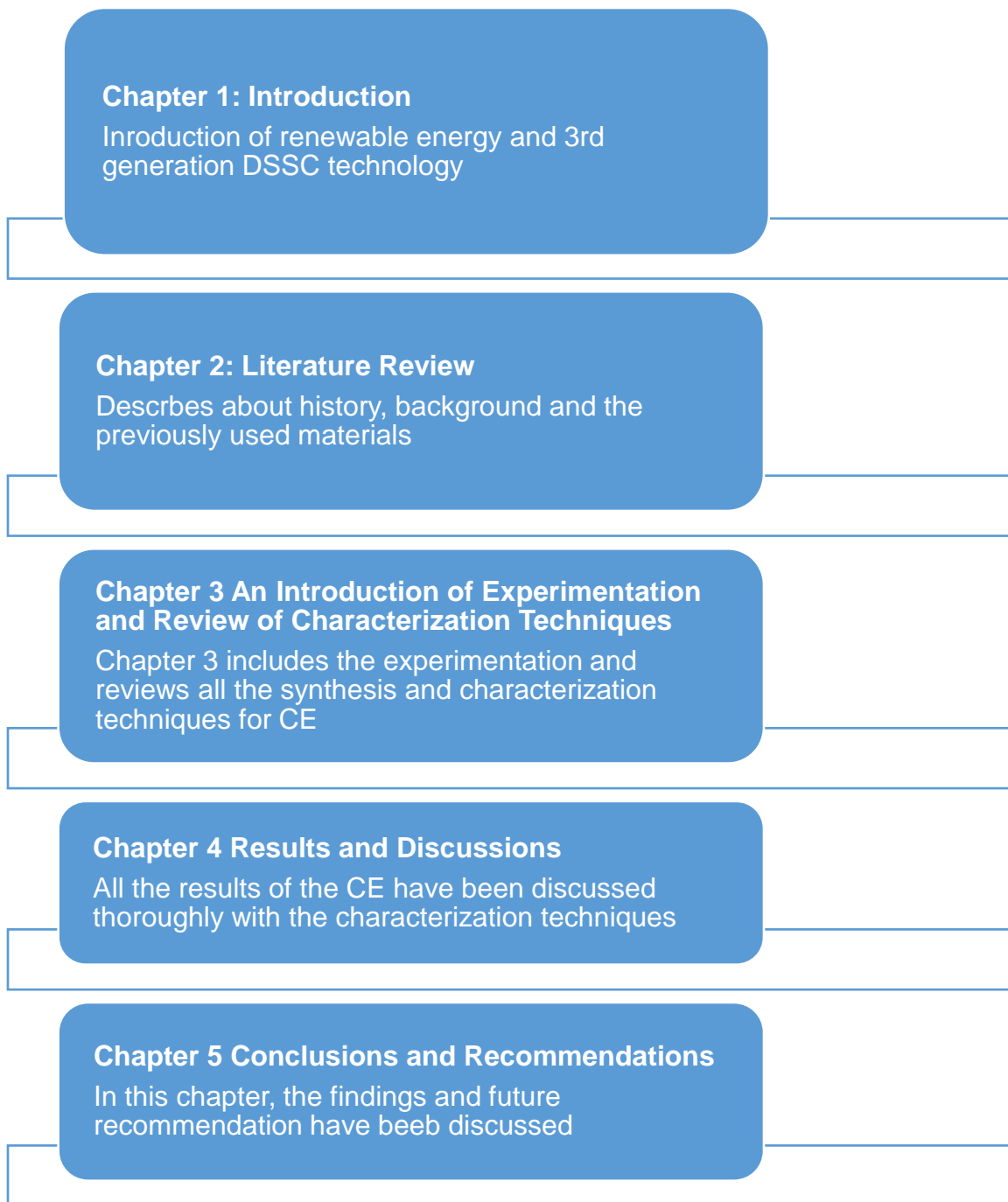


Figure 1-9 Diagram depicting flow of thesis

1.9 Scope of Thesis

Pakistan is an energy-scarce country, 70% of energy is coming from fossil fuels, by doing work on renewable energy sources and their relevant techniques, will promote the renewable energy trend as well as we have a lot of potential for solar energy as we lie on the solar belt. So, in that way, this research not only fulfills our energy needs but will reduce our dependency on the usage of fossil fuels.

The thesis primarily comprises three stages, such as synthesis of the proposed material, characterizing the materials with different techniques, and then analyzing their results. In the first stage, carbon-doped titania was synthesized through hydrothermal synthesis followed by calcination in the tube furnace. Then prepared samples were coated on the FTO slides with the help of the doctor blade technique coating method. In the second stage, all the prepared samples were characterized with the help of the following techniques like X-ray diffraction (XRD), scanning electron microscope (SEM), Energy-dispersive X-ray spectroscopy (EDS), and Raman spectroscopy. Afterward, samples were analyzed through the cyclic voltammetry (CV) and I-V characteristic curve (IV) to know the performance and efficiency of the fabricated CEs in the dye-sensitized solar cells. From the results obtained from the C-TiO₂-based DSSC, it's been observed that the kinetics of the cell have been improved and exhibit comparable photoconversion efficiencies in comparison to Pt.

Summary

Chapter 1 briefly describes the importance of renewable energy sources especially solar energy due to their large potential all over the world. Due to the rise in global temperature and climate change phenomenon, time requires to shift to renewable energy sources because they don't emit greenhouse gases into the atmosphere, are the inexhaustible source, and environmentally friendly and have large potential across the globe, on the other hand, fossil fuels are responsible for ozone layer depletion, acid rain occurs, glaciers are being melted, temperature rise and other harmful effects. According to World Bank, only 1.5% of the solar potential is being used which is too low, and more focus should be given to this side.

The concept of solar energy, photovoltaic technology, and other related terminologies in the solar cell are explained in detail. All the generations of solar cells were also described with their characteristics and a special focus on the cell, dye-sensitized solar cell with their basic principle of working, components, and their applications, as well as the features that give this generation edge over the other generation of solar cells.

In last, I have defined the objectives of my research, alternative materials that have been used previously, challenges in the CE field, and the properties of my proposed carbon-doped titania CE in the DSSCs.

References

- [1] “Knowledge, perception and awareness of renewable energy by engineering students in Nigeria: A need for the undergraduate engineering program adjustment | Elsevier Enhanced Reader.”
- [2] A. Harjanne and J. M. Korhonen, “Abandoning the concept of renewable energy,” *Energy Policy*, vol. 127, no. December 2018, pp. 330–340, 2019.
- [3] H. Lund, “Renewable energy strategies for sustainable development,” *Energy*, vol. 32, pp. 912–919, 2007.
- [4] W. Wang, L. W. Fan, and P. Zhou, “Evolution of global fossil fuel trade dependencies,” *Energy*, vol. 238, p. 121924, 2022.
- [5] H. van Asselt, “Governing fossil fuel production in the age of climate disruption: Towards an international law of ‘leaving it in the ground,’” *Earth Syst. Gov.*, vol. 9, p. 100118, 2021.
- [6] R. E. N. Members, *Renewables 2021 global status report 2021*. 2021.
- [7] “When Fossil Fuels Run Out, What Then? - MAHB.” [Online]. Available: <https://mahb.stanford.edu/library-item/fossil-fuels-run/>. [Accessed: 11-Jan-2022].
- [8] I. Energy Agency, “Renewables 2021 - Analysis and forecast to 2026,” 2021.
- [9] “Solar energy potential assessment: A framework to integrate geographic, technological, and economic indices for a potential analysis | Elsevier Enhanced Reader.”
- [10] “Solar Photovoltaic Power Potential by Country.” [Online]. Available: <https://www.worldbank.org/en/topic/energy/publication/solar-photovoltaic-power-potential-by-country>. [Accessed: 11-Jan-2022].
- [11] “The linkage between renewable energy potential and sustainable development: Understanding solar energy variability and photovoltaic power potential in Tibet, China | Elsevier Enhanced Reader.”
- [12] “Passive Solar History.” [Online]. Available: <http://californiasolarcenter.org/old->

pages-with-inbound-links/history-pv/. [Accessed: 13-Jan-2022].

- [13] M. Taguchi, A. Suzuki, N. Ueoka, and T. Oku, “The History of Solar,” *AIP Conf. Proc.*, vol. 2067, 2019.
- [14] “Solar Photovoltaic Technology Basics | NREL.” [Online]. Available: <https://www.nrel.gov/research/re-photovoltaics.html>. [Accessed: 13-Jan-2022].
- [15] “How a Solar Cell Works - American Chemical Society.”
- [16] “(20) (PDF) Temperature Effect on Power Drop of Different Photovoltaic Modules.”
- [17] “Method to determine the single curve IV characteristic parameter of solar cell.”
- [18] S. Ananthakumar, J. R. Kumar, and S. M. Babu, “Third-Generation Solar Cells: Concept, Materials and Performance - An Overview,” pp. 305–339, 2019.
- [19] K. Sharma, V. Sharma, and S. S. Sharma, “Dye-Sensitized Solar Cells: Fundamentals and Current Status.”
- [20] Y.-H. Fan, C.-Y. Ho, and Y.-J. Chang, “Enhancement of Dye-Sensitized Solar Cells Efficiency Using Mixed-Phase TiO₂ Nanoparticles as Photoanode,” 2017.
- [21] Mitch Jacoby, “Commercializing low-cost solar cells,” *C&EN Glob. Enterp.*, vol. 94, no. 18, pp. 30–35, May 2016.
- [22] F. Yu, Y. Shi, W. Yao, S. Han, and J. Ma, “A new breakthrough for graphene/carbon nanotubes as CEs of dye-sensitized solar cells with up to a 10.69% power conversion efficiency,” *J. Power Sources*, vol. 412, no. October 2018, pp. 366–373, 2019.
- [23] S. A. Almohsin, M. Mohammed, Z. Li, M. A. Thomas, K. Y. Wu, and J. B. Cui, “Multi-walled carbon nanotubes as a new CE for dye-sensitized solar cells,” *J. Nanosci. Nanotechnol.*, vol. 12, no. 3, pp. 2374–2379, 2012.
- [24] “Synergetic Effects of Hybrid Carbon Nanostructured CEs for Dye.pdf.”
- [25] S. Farooq, A. A. Tahir, U. Krewer, A. ul H. A. Shah, and S. Bilal, “Efficient

photocatalysis through conductive polymer coated FTO CE in platinum free dye sensitized solar cells,” *Electrochim. Acta*, vol. 320, p. 134544, 2019.

- [26] C. Wu, G. Li, X. Cao, B. Lei, and X. Gao, “Carbon nitride transparent CE prepared by magnetron sputtering for a dye-sensitized solar cell,” *Green Energy Environ.*, vol. 2, no. 3, pp. 302–309, 2017.
- [27] S. Prasad *et al.*, “3D nanorhombus nickel nitride as stable and cost-effective CEs for dye-sensitized solar cells and supercapacitor applications,” *RSC Adv.*, vol. 8, no. 16, pp. 8828–8835, 2018.
- [28] U. Ahmed, M. Alizadeh, N. Abd, S. Shahabuddin, M. Shakeel, and A. K. Pandey, “A comprehensive review on CEs for dye sensitized solar cells : A special focus on Pt-TCO free CEs,” *Sol. Energy*, vol. 174, no. October, pp. 1097–1125, 2018.
- [29] Ş. Sungur, “Titanium Dioxide Nanoparticles,” *Handb. Nanomater. Nanocomposites Energy Environ. Appl.*, pp. 713–730, 2021.

Chapter 2: Literature Review

2.1 Background of DSSC

In the 19th century, the first time photovoltaic effect was observed by a French scientists Alexandria-Edmond, paved the way and provide foundation towards the discovery of solar cell[1]. He observed this phenomenon during an experiment when two Pt based electrodes were soaked in halide salt based electrolyte solution, electric current was generated when this apparatus exposed to the sunlight. In 1960s, another development was to generation of electricity by exposing sunlight onto the organic dyes in the semiconductor based devices[2]. Later this, phenomenon of photoexcitation were studied to simulate the mechanism of photosynthesis at the University of California. In 1980s, it was reported that efficiency of the DSSC can be enhanced by tuning or changing the porosity of semiconductor oxide material[3]. By having an edge over conventional PV technology, after extensive research and experimentation, first DSSC was developed in 1991 by O'Regan and Gratzel having very low efficiency[4]. The concept of DSSC was the same as process takes place during photosynthesis in plants. By incorporation and utilization of different and novel material are used in DSSC to enhance the efficiency. Usage of different materials as CE have been clearly shown in Table 1, indicating the relevant parameters of solar cell and have different efficiencies respectively.

2.2 Basic Structure of DSSC

DSSCs belong to 3rd generation based solar cells. Primarily it consists of the following components, which are clearly shown in Figure 2-1[5].

- Conductive glass substrate
- Working electrode/Photoanode
- Dyes
- Electrolytes
- CE

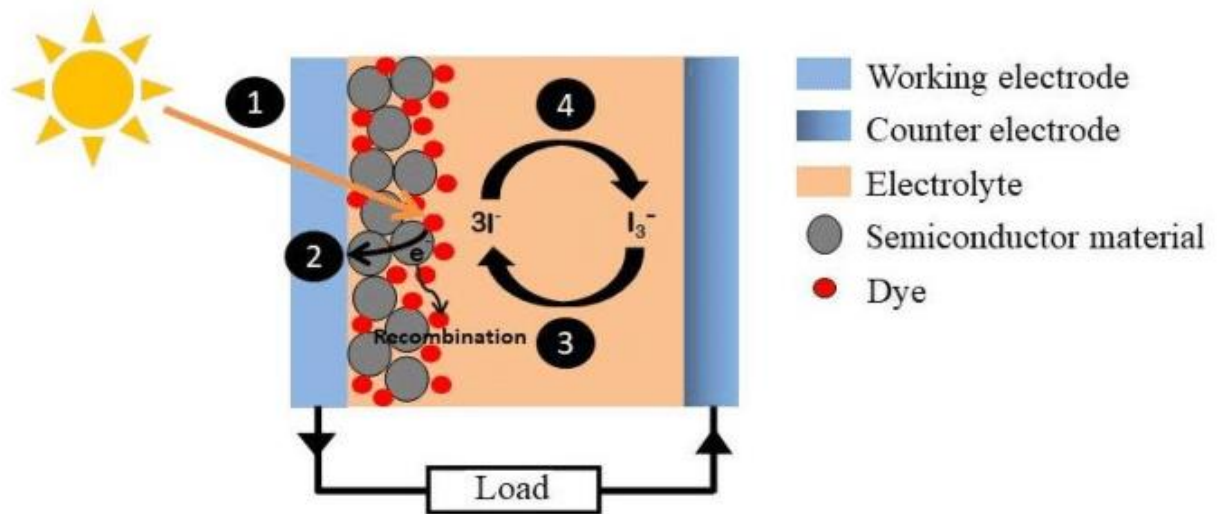


Figure 2-1 Basic structure / components of dye sensitized solar cell

2.2.1 Conductive glass substrates

These glass substrates are highly conductive and have very less resistance of value $20 \Omega/\text{sq.}$ to pass the current, that is being generated from the dye molecules that are becomes excited and eject electron in the conduction band from valence band, when energy packets in form of photon strikes. They are used as substrates for both the CE as well as for the photoanode/ working electrode. They are also called current carrier as current is passed through the glass substrates, following the external circuit, and reaches to the CE to complete the cycle of electron flow. Glass substrates are further classified into two types

- Indium doped tin oxide (ITO)
- Fluorine doped tin oxide (FTO)

There are also many other glass substrates present, but having good properties to be employed in solar cells, mostly ITO and FTO are used for research purposes. Both of the glass substrates are used according to the application, as both have different characteristics. ITO is quite expensive, has less reflectance than FTO, as well as is less tolerable to temperature than FTO. FTOs have high thermal stability and high resistance to corrosion.

2.2.2 Working Electrode / Photoanode

Working electrode in the DSSC consists of dye molecules adsorbed on semiconductor based oxide materials such as titania or titanium dioxide coated on the glass substrates, used for the charge transportation. Mostly, anatase phase of the TiO_2 is used for the DSSC applications having a band gap of 3.2eV, as well as it is relatively cheap, inexpensive and abundantly present in the earth's crust. Titania paste are made by incorporating the binders, so that it may form a strong bond with the surface of glass substrates. Various coating methods like doctor blade or screen printing used to coat the paste onto the substrate surfaces. The binder is removed after being heat at 400-450C for half an hour, so that all the binder materials is removed and no impurities present over there. Simply, nanoparticles are completely attached to the surface of the conductive substrates. Depending upon the crystallinity and structure of the TiO_2 nanoparticles, these are further classified into three phases, such as rutile, anatase and brookite phase. Each of them has different crystallinity and structure and employed in different applications accordingly. Not only titanium oxide materials are used in DSSC, while other metal oxide materials are also used for DSSC applications such as ZnO , SiO_2 , Zn_2SnO_4 , CeO_2 , WO_3 , SrTiO_3 , and Nb_2O_5 . Different material showed different photo conversion efficiency as they have different properties to each other. In the abovementioned photoanode materials, the ZnO nanoparticles showed better efficiency with higher charge transportation as it has band gap close to the TiO_2 , and can replace the TiO_2 effectively. However many issues are still over there such as recombination losses and other related issues, scientists are trying to address all the issues by incorporating and inventing new alternative materials, so that efficiency of the DSSC can be improved that will help it out in commercialization.

2.2.3 Dyes

Dyes are the organic molecules that are used in DSSCs as a sensitizer, which are responsible for the excitation and generation of electrons when dye is exposed to the sunlight. Dye is adsorbed on the photoanode and plays an important role in the solar cell. Dyes absorb visible spectra ranging from 400-700nm and can be adsorbed onto the titania in DSSCs. Strong anchoring groups in the dyes are responsible for strong adsorption with the photoanode. The HOMO level of the dyes should be higher than the HOMO level of the titania nanoparticles, otherwise chances of recombination increased. Various dye

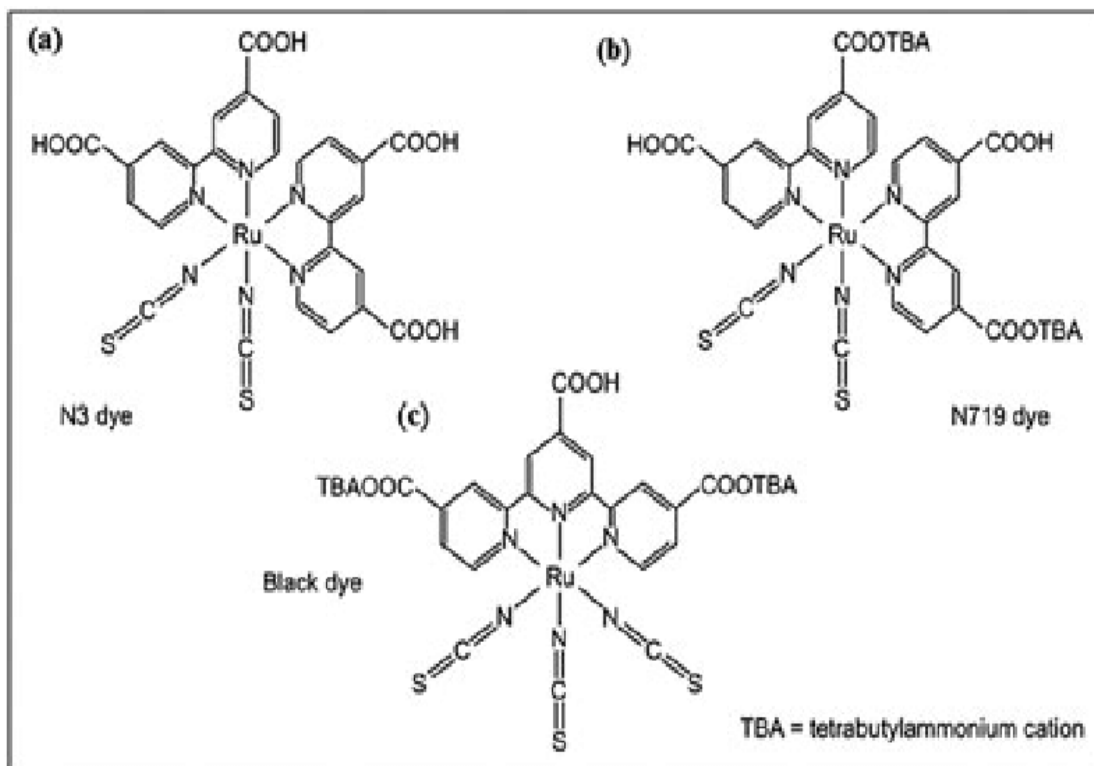


Figure 2-2 Basic molecular structure of a) N3 dyes b) N719 dyes c) black dyes

molecules are being used such as N719, N3, black dyes etc. can be shown in Figure 2-2 [6] to enhance efficiency, because the main problem by using dyes is their degradation, when these cells are placed in ambient conditions then dye degrades and the overall cell performance becomes unsatisfactory. Stability issues in the dyes should be addressed for better performance leading towards a long life.

2.2.4 Electrolytes

Electrolyte in DSSC is another key component that act as a medium between photoanode and CE, and complete the cycle of charge transportation, starting from generation from dye molecules, transporting through the titania nanoparticles, flowing through the external circuit to the CE and reduction of triiodide ions and then iodide ions. In that redox mediator plays an important role to regenerate the dye molecules for further excitation. Usually redox mediator consists of iodide ions and triiodide ions, which forms during oxidation and reduction mechanism. A good electrolyte should be chemically active and of reversible in nature and should have minimum viscosity towards the diffusion of charges, low recombination losses, optimum boiling properties, and dielectric properties,

so that redox reactions takes place rapidly and process continues. It should also have less corrosive properties and should be optimally viscous, so that it may not create leakage problems. Electrolytes are further classified into three different categories such as

- Liquid electrolytes
- Solid electrolytes
- Quasi solid state electrolytes

2.2.4.1 Liquid Electrolytes

In a study reported, for the first time efficiency 7-8% of the DSSC by using iodide/triiodide organic liquid electrolyte. Liquid electrolytes have many benefits over others, such as low viscosity, highly conductive, excellent interconnected properties between electrolyte and the electrode, less corrosive and most importantly they have simple preparation methods etc. that's why they showed good overall cell efficiency. Maximum reported efficiency of the DSSC greater than 14% of DSSC have been achieved by using the liquid electrolyte[7]. In the liquid electrolytes, the leakage happened due to low viscosity of electrolytes, that is the main limitation of liquid electrolytes. Though, this issue has also being addressed by employing innovative electrolyte materials to compensate this adverse effect, to enhance the overall performance of the cell. Liquid electrolytes are further classified into solvents and redox mediators, while solvent liquid electrolyte are further divided into organic and ionic liquid electrolyte, and redox mediator are into two iodide/triiodide redox couple and free mediators.

2.2.4.2 Quasi-Solid State Electrolytes

Quasi solid state are the electrolytes that are present between liquid and solid. They consists of polymer host filled with liquid electrolyte. To cater the leakage issues of electrolytes in DSSC, quasi-solid state electrolyte or also called gel electrolyte, is most effective alternative for the stable DSSC. Usually, they have very good ionic conductivity, simple preparation procedure, and good chemical properties for the charge transportation. Another advantage of using gel electrolyte due to their high viscosity, which makes it compatible for deposition methods leading to cheaper DSSC. As they compensate the limitations incur in liquid electrolytes, they show good stability and charge transfer properties.

2.2.4.3 Solid electrolytes

Leakage issues in both of the above mentioned electrolytes, solid electrolytes are responsible to compensate leakage. It is the main motivation of the most of the scientists, to develop a solid DSSC to improve the efficacy. As they are solid in nature and not include solvents, so there are no corrosion and leakage problems at all. A lot of solid conducting material are being used and invented such as, ionic conductors, inorganic hole-transport materials, and organic hole-transport materials.

2.2.5 Counter Electrode

CE is an important component of the DSSC. Its physical and chemical properties matters a lot for the function and process of the cell. CE has these following functions during the cell working. First one, a) it completes the cycle of electrons that was produced at the photoanode as well as reduced the redox couple at the surface of CE by accepting electron. As CE reduce the redox couple, then the ions present in the electrolyte reduces the oxidized dye in its original form. Second function b) is like a medium, as it accepts electron from the external circuit and reduce the electrolyte solution present, so its works like a connector and complete the cycle. Third one is, c) it performs like a good reflector, as unabsorbed light or photons are reflect back towards the working electrode, so that optimum efficiency of the cell can be achieved.

To perform all of the abovementioned functions, a CE should have good catalytic activity, highly conductive, high surface area with porous structure, resistance towards corrosion, reflective properties as well as good bonding properties with the transparent conductive oxide that acts as a contact in the cell. To achieve all of the abovementioned properties of a CE in a single material is quite impossible. Actually, Pt as a CE fulfills the properties, as it is highly catalytic active and conductive material with countless cycles of working in the cycle and having long life, but the issue of employing Pt is of their high cost and rare presence in nature, that makes device quite expensive.

2.2.5.1 Counter Electrode materials for DSSCs

Due to high cost and rarity of Pt metal, researches are trying to find out competitive alternatives for better catalytic activity and efficiency of the DSSC, such as carbonaceous materials, conducting polymers, metal oxide and sulfides. Carbonaceous based materials

have an edge over other materials due to their associated benefits such as low cost, abundantly available in nature, high conductivity, and corrosion towards the iodine and high catalytic activity towards the triiodide ion reduction. Pt can be replaced with other materials that have been explained in the table. Gratzel developed carbon based CE in 1996, a graphitic–carbon black mixture with a photo conversion efficiency (PCE) of 6.7 percent. In 2008, it was reported that using Nano-sized carbon as a CE resulted in a power conversion efficiency of 7.56 percent. The photo conversion efficiency of spray coated carbon was found to be 6.2 percent. In comparison to others, mesoporous carbon has a high PCE of 7.5 percent. The PCE of carbon nanofibers was investigated at temperatures ranging from 550 to 750 degrees Celsius, and it was discovered to be higher at 550 degrees Celsius. Wang reported a PCE of 7.02 percent when he used nitrogen-doped mesoporous carbon (NMC) as the CE. Graphene also used in fuel cells due to its charge charge transferring features. Graphene with carbon black exhibits showed 5.99 % PCE. In comparison to graphene-SWCNT CE, graphene-based CE had a higher PCE of 5.87 %. Researchers chose carbonaceous material to replace Pt-based CEs because of its cost effectiveness and availability. The use of carbonaceous CEs for long periods of time is limited due to some disadvantages, such as the poor connection of carbon film to TCO and the need huge quantity to achieve the best activity. Table 2.1 showed all the different CE material, included carbonaceous CEs, used in the cell from its discovery to up till now, all the CE materials showed the open circuit voltage V_{oc} , short circuit current I_{sc} , fill factor FF, and photo conversion efficiencies.

Table 2-1 History of DSSC’s based upon different CE materials

Sr. No	CE	J_{sc} (mA cm^{-2})	V_{oc} (V)	FF	PCE (%)	Year	Ref.
1	Carbon black powder	11.3	0.82	0.71	6.67	1996	[8]
2	Carbon black	16.8	0.79	0.68	9.10	2006	[9]
3	PANI	14.6	0.17	0.69	7.15	2008	[10]
3	Carbon	16.5	0.07	0.64	7.56	2008	[11]

4	Pure carbon	13.1	0.70	0.70	6.46	2009	[12]
5	Glassy carbon	19.3	0.66	0.45	5.78	2011	[13]
6	NbO ₂	13.9	0.81	0.70	7.88	2011	[14]
7	WO ₂	14.0	0.80	0.64	7.25	2011	[15]
8	MoS ₂	13.8	0.76	0.73	7.59	2011	[16]
9	WS ₂	14.1	0.78	0.70	7.73	2011	[16]
10	Graphene	13.1	0.70	63.6	5.87	2012	[17]
11	Carbon 300s	12.7	0.81	0.54	5.60	2012	[18]
12	Carbon 420s	13.1	0.81	0.57	6.20	2012	[18]
13	TaO	12.5	0.77	0.67	6.48	2012	[19]
14	Transparent carbon	10.5	0.72	0.60	6.07	2013	[20]
15	PEDOT	16.2	0.71	0.61	7.04	2013	[21]
16	ZnO/Polymer	19.7	0.86	0.48	8.17	2013	[22]
17	Carbon nanofiber	7.4	0.71	0.42	2.17	2014	[23]
18	Nanofiber PANI	14.7	0.72	0.59	6.21	2014	[24]
19	Fe ₃ O ₄	16.6	0.69	0.63	7.65	2014	[25]
20	RuO ₂	16.5	0.81	0.54	7.22	2014	[26]
21	FTO/Au/GNP	18.3	1.01	0.77	14.3	2015	[27]
22	rGO/PANI	11.6	0.52	0.47	2.93	2016	[28]
23	rGO/PEDOT	10.6	0.49	0.38	2.05	2016	[28]
24	MoS ₂ /CNTs	16.6	0.74	0.66	7.83	2017	[29]
25	PANI-G1C ₂	18.2	0.78	0.54	7.67	2017	[30]
26	PEDOT-40s	13.7	0.77	0.63	6.77	2017	[31]
27	FeS	14.0	0.66	0.63	6.47	2017	[32]
28	CoS/MoS ₂	16.5	0.74	0.61	7.48	2018	[33]

29	CO ₃ nanosheets/rGO	15.7	0.75	0.67	8.08	2018	[34]
30	MoSe ₂	13.9	0.76	0.67	6.83	2019	[35]
31	Electrodeposited MoS ₂	12.4	0.62	0.61	4.35	2020	[36]
32	Cu ₂ ZnS ₄	13.4	0.73	0.67	6.19	2021	[37]

DSSC is a promising and viable technique and having advantages over other generation of solar cell such as simple fabrication procedure, cost effective, environmental friendly as well as lower in weight. Hydrothermal synthesis and in situ/ oxidative polymerization methods are usually used to fabricate the CEs, and doctor blade coating used to coat material onto the conductive oxides, though doctor blade is easy and time saving technique, but films thickness can't be controlled through doctor blade coating method, so for this different coating techniques should be used to control thickness such as spin coating, screen printing, and PED are preferable options for coating. Carbonaceous materials as CE showed good electrocatalytic and stability properties, while conductive polymers show good conductive as well as less resistance charge transfer resistance values. So, in future a CE material comprising of carbonaceous-conducting polymer material based CE should be investigated to form cost effective and efficient DSSC.

DSSC has the equivalent cost as the thin films solar cells have. As compared to silicon first generation solar cell technology, they can be easily fabricate with less energy intensive process as well as less emissions into the atmosphere leads to cost effective solar cell, that makes this technology another step closer to commercialization.

Summary

In this chapter, the history of solar cell invention and all the derivation in the way of third generation DSSCs are briefly discussed, as well as all the components of the DSSC have been discussed in detail, their properties, their functions in the cell, and their performance. Normally due to the superior catalytic and conductive properties, Pt is taken as standard. Though it showed good performance and high photo conversion efficiencies of the cell, but due to its high cost, different material came into consideration and all the CE materials such as carbonaceous, metal sulphides, metal nitrides, complex conductive polymer, that are being used and been reported, due to their extraordinary properties like highly conductivity, stability and cost effective materials. All the alternative materials have potential to replace Pt metal CE due to their comparative photo conversion efficiencies such as V_{oc} , J_{sc} , FF and efficiencies that have been reported in the table.

References

- [1] “Dye-sensitized Solar Cells – materiability.” [Online]. Available: <http://materiability.com/dye-sensitized-solar-cells/>. [Accessed: 04-Feb-2022].
- [2] H. Gerischer, M. E. Michel-Beyerle, F. Reberndorf, and H. Tributsch, “Sensitization of charge injection into semiconductors with large band gap,” *Electrochim. Acta*, vol. 13, no. 6, pp. 1509–1515, 1968.
- [3] M. Matsumura, S. Matsudaira, H. Tsubomura, M. Takata, and H. Yanagida, “Dye Sensitization and Surface Structures of Semiconductor Electrodes,” *Ind. Eng. Chem. Prod. Res. Dev.*, vol. 19, no. 3, pp. 415–421, Sep. 2002.
- [4] G. Boschloo, “Improving the performance of dye-sensitized solar cells,” *Front. Chem.*, vol. 7, no. FEB, p. 77, 2019.
- [5] N. Jamalullail, I. S. Mohamad, M. N. Norizan, N. Mahmed, and B. N. Taib, “Erratum to: Recent improvements on TiO₂ and ZnO nanostructure photoanode for dye sensitized solar cells: A brief review (EPJ Web of Conferences (2017) 162 (01045) DOI: 10.1051/epjconf/201716201045),” *EPJ Web Conf.*, vol. 162, Nov. 2017.
- [6] S. Shalini, R. Balasundaraprabhu, T. Satish Kumar, N. Prabavathy, S. Senthilarasu, and S. Prasanna, “Status and outlook of sensitizers/dyes used in dye sensitized solar cells (DSSC): a review,” *Int. J. Energy Res.*, vol. 40, no. 10, pp. 1303–1320, Jan. 2016.
- [7] K. Kakiage, Y. Aoyama, T. Yano, K. Oya, J. I. Fujisawa, and M. Hanaya, “Highly-efficient dye-sensitized solar cells with collaborative sensitization by silyl-anchor and carboxy-anchor dyes,” *Chem. Commun.*, vol. 51, no. 88, pp. 15894–15897, Oct. 2015.
- [8] A. Kay and M. Grätzel, “Low cost photovoltaic modules based on dye sensitized nanocrystalline titanium dioxide and carbon powder,” *Sol. Energy Mater. Sol. Cells*, vol. 44, no. 1, pp. 99–117, Oct. 1996.
- [9] T. N. Murakami *et al.*, “Highly Efficient Dye-Sensitized Solar Cells Based on

- Carbon Black CEs,” *J. Electrochem. Soc.*, vol. 153, no. 12, p. A2255, 2006.
- [10] Q. Li *et al.*, “Application of microporous polyaniline CE for dye-sensitized solar cells,” *Electrochem. commun.*, vol. 10, no. 9, pp. 1299–1302, Sep. 2008.
- [11] W. J. Lee, E. Ramasamy, D. Y. Lee, and J. S. Song, “Performance variation of carbon CE based dye-sensitized solar cell,” *Sol. Energy Mater. Sol. Cells*, vol. 92, no. 7, pp. 814–818, Jul. 2008.
- [12] J. Chen *et al.*, “A flexible carbon CE for dye-sensitized solar cells,” *Carbon N. Y.*, vol. 47, no. 11, pp. 2704–2708, Sep. 2009.
- [13] S. Xu, Y. Luo, and W. Zhong, “Investigation of catalytic activity of glassy carbon with controlled crystallinity for CE in dye-sensitized solar cells,” *Sol. Energy*, vol. 85, no. 11, pp. 2826–2832, Nov. 2011.
- [14] X. Lin, M. Wu, Y. Wang, A. Hagfeldt, and T. Ma, “Novel CE catalysts of niobium oxides supersede Pt for dye-sensitized solar cells,” *Chem. Commun.*, vol. 47, no. 41, pp. 11489–11491, Nov. 2011.
- [15] M. Wu, X. Lin, A. Hagfeldt, and T. Ma, “A novel catalyst of WO₂ nanorod for the CE of dye-sensitized solar cells,” *Chem. Commun.*, vol. 47, no. 15, pp. 4535–4537, Mar. 2011.
- [16] M. Wu *et al.*, “Economical and effective sulfide catalysts for dye-sensitized solar cells as CEs,” *Phys. Chem. Chem. Phys.*, vol. 13, no. 43, pp. 19298–19301, Nov. 2011.
- [17] H. J. Kim, G. Rooh, S. Kim, and S. J. Kang, “Cs₂Li(Na)Gd(1-x)Ce_xCl(Br) crystal scintillators for radiation detection,” *Procedia Eng.*, vol. 32, pp. 53–59, 2012.
- [18] G. Veerappan, K. Bojan, and S. W. Rhee, “Amorphous carbon as a flexible CE for low cost and efficient dye sensitized solar cell,” *Renew. Energy*, vol. 41, pp. 383–388, May 2012.
- [19] S. Yun, L. Wang, W. Guo, and T. Ma, “Non-Pt CE catalysts using tantalum oxide for low-cost dye-sensitized solar cells,” *Electrochem. commun.*, vol. 24, no. 1, pp.

69–73, Oct. 2012.

- [20] C. Bu *et al.*, “Highly transparent carbon CE prepared via an in situ carbonization method for bifacial dye-sensitized solar cells,” *ACS Appl. Mater. Interfaces*, vol. 5, no. 15, pp. 7432–7438, Aug. 2013.
- [21] X. Yin *et al.*, “Facile synthesis of poly(3,4-ethylenedioxythiophene) film via solid-state polymerization as high-performance Pt-free CEs for plastic dye-sensitized solar cells,” *ACS Appl. Mater. Interfaces*, vol. 5, no. 17, pp. 8423–8429, Sep. 2013.
- [22] H. Wang, W. Wei, and Y. H. Hu, “Efficient ZnO-based CEs for dye-sensitized solar cells,” *J. Mater. Chem. A*, vol. 1, no. 22, pp. 6622–6628, Jun. 2013.
- [23] D. Sebastián, V. Baglio, M. Girolamo, R. Moliner, M. J. Lázaro, and A. S. Aricò, “Carbon nanofiber-based CEs for low cost dye-sensitized solar cells,” *J. Power Sources*, vol. 250, pp. 242–249, Mar. 2014.
- [24] Y. Xiao, G. Han, Y. Li, M. Li, and Y. Chang, “High performance of Pt-free dye-sensitized solar cells based on two-step electropolymerized polyaniline CEs,” *J. Mater. Chem. A*, vol. 2, no. 10, pp. 3452–3460, Mar. 2014.
- [25] L. Wang, Y. Shi, H. Zhang, X. Bai, Y. Wang, and T. Ma, “Iron oxide nanostructures as highly efficient heterogeneous catalysts for mesoscopic photovoltaics,” *J. Mater. Chem. A*, vol. 2, no. 37, pp. 15279–15283, Oct. 2014.
- [26] Y. Hou *et al.*, “Highly electrocatalytic activity of ruo2 nanocrystals for triiodide reduction in dye-sensitized solar cells,” *Small*, vol. 10, no. 3, pp. 484–492, Feb. 2014.
- [27] K. Kakiage, Y. Aoyama, T. Yano, K. Oya, J.-I. Fujisawa, and M. Hanaya, “Chemical Communications Highly-efficient dye-sensitized solar cells with collaborative sensitization by silyl-anchor and carboxy-anchor dyes,” 2015.
- [28] R. Li, Q. Tang, L. Yu, X. Yan, Z. Zhang, and P. Yang, “CEs from conducting polymer intercalated graphene for dye-sensitized solar cells,” *J. Power Sources*, vol. 309, pp. 231–237, Mar. 2016.

- [29] C. H. Lin, C. H. Tsai, F. G. Tseng, C. C. M. Ma, H. C. Wu, and C. K. Hsieh, “Three-dimensional vertically aligned hybrid nanoarchitecture of two-dimensional molybdenum disulfide nanosheets anchored on directly grown one-dimensional carbon nanotubes for use as a CE in dye-sensitized solar cells,” *J. Alloys Compd.*, vol. 692, pp. 941–949, 2017.
- [30] Y. C. Shih, H. L. Lin, and K. F. Lin, “Electropolymerized polyaniline/graphene nanoplatelet/multi-walled carbon nanotube composites as CEs for high performance dye-sensitized solar cells,” *J. Electroanal. Chem.*, vol. 794, pp. 112–119, Jun. 2017.
- [31] J. Ma, S. Qingfeng, Z. Fengbao, and W. Mingxing, “Improvement on the catalytic activity of the flexible PEDOT CE in dye-sensitized solar cells,” *Mater. Res. Bull.*, vol. 100, pp. 213–219, Apr. 2018.
- [32] C. Zhang, L. Deng, P. Zhang, X. Ren, Y. Li, and T. He, “Electrospun FeS nanorods with enhanced stability as CEs for dye-sensitized solar cells,” *Electrochim. Acta*, vol. 229, pp. 229–238, Mar. 2017.
- [33] X. Wang *et al.*, “The sesame ball-like CoS/MoS₂ nanospheres as efficient CE catalysts for dye-sensitized solar cells,” *J. Alloys Compd.*, vol. 739, pp. 568–576, Mar. 2018.
- [34] T. Jiang *et al.*, “Economic synthesis of Co₃S₄ ultrathin nanosheet/reduced graphene oxide composites and their application as an efficient CE for dye-sensitized solar cells,” *Electrochim. Acta*, vol. 261, pp. 143–150, Jan. 2018.
- [35] X. Cao, H. Li, G. Li, and X. Gao, “Electrocatalytically active MoSe₂ CE prepared in situ by magnetron sputtering for a dye-sensitized solar cell,” *Chinese J. Catal.*, vol. 40, no. 9, pp. 1360–1365, Sep. 2019.
- [36] M. Gurulakshmi *et al.*, “Electrodeposited MoS₂ CE for flexible dye sensitized solar cell module with ionic liquid assisted photoelectrode,” *Sol. Energy*, vol. 199, pp. 447–452, Mar. 2020.
- [37] “Sci-Hub | In situ solvothermal growth of Cu₂ZnSnS₄ thin film for CE of dye-

sensitized solar cells. Solid State Sciences, 113, 106547 | 10.1016/j.solidstatesciences.2021.106547.” [Online]. Available: <https://sci-hub.hkvisa.net/https://www.sciencedirect.com/science/article/abs/pii/S1293255821000169>. [Accessed: 01-Feb-2022].

Chapter 3: An Introduction of Experimentation and Review of Characterization Techniques

3.1 Experimentation

C-TiO₂ CEs were prepared through the hydrothermal synthesis followed by calcination in the tube furnace to get the CE powder. C-TiO₂ powder further mixed with DI water and absolute alcohol with appropriate ratios to form paste that is further coated onto the conductive glass substrate by using the doctor blade coating method to form thin films, after that films were kept in dry oven so that volatile substance leave the pure thin films on the substrate.

3.1.1 Synthesis of carbon-doped titania powder material

Figure 3-1 shows all the synthesis clearly and step by step. Titanium (IV) oxide (TiO₂), Anatase (Daejung, above 98%), and Glucose monohydrate (C₆H₁₂O₆.H₂O) Sigma Aldrich USA, materials were used to synthesize C-TiO₂ powder material to be used as a CE for dye-sensitized solar cell applications through the hydrothermal synthesis method as shown in Figure 3-2. The precursors, 0.25g (5% of titania) of glucose monohydrate, 5g of

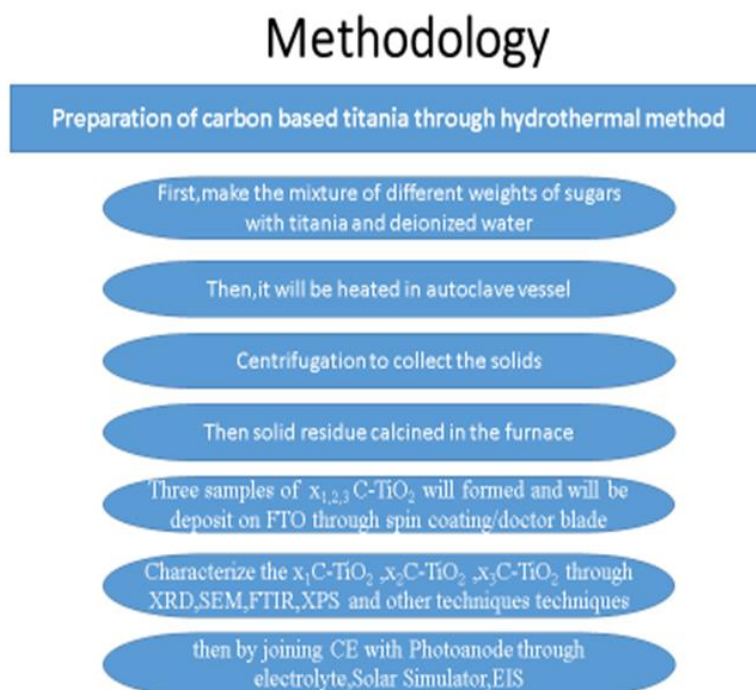


Figure 3-1 Method to be followed for the fabrication of CE

titania anatase, and 9ml of deionized water were properly mixed through the magnetic stirring(VELP Scientifica) under 400rpm for 30 minutes.

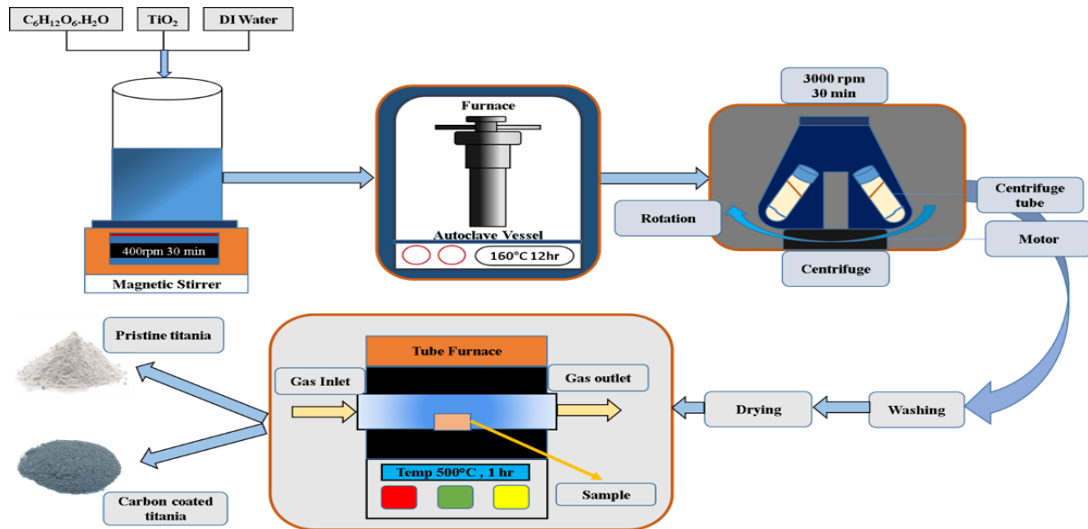


Figure 3-2 Synthesis of carbon doped titania CE followed by calcination in the tube furnace

After that, the solution was heated (High-performance Oven, USA Sheldon) in a 50 ml autoclave vessel at 160 °C for 12 hours to get highly crystalline materials[12]. The suspension in the autoclave vessel was then centrifuged (centrifuge model 800) at 3000 rpm for 30 min to collect the solids after the successful separation of particles from solution, that accumulated on the bottom of the falcon tubes. Then solid residue was calcined in the tube furnace (GSL-1600X-100LD, MTI USA) to form C-TiO₂ powders at 500 °C for 1hr under argon gas flow. The other C-TiO₂ powders were also prepared using same method by varying the amount of glucose.monohydrate 0.5 g (10 % of TiO₂), 0.75 g (15 % of TiO₂), and 1g (20 % of TiO₂) against 5 g of anatase titania.

3.1.2 Fabrication of CE

Synthesized powders of different carbon to titania ratios were mixed with DI water and absolute alcohol to make the paste followed by stirring under 3000 rpm for 30 minutes. After making the paste, doctor blade coating method was used to coat the paste onto the FTO glass substrate. FTO Paste coated glass substrates were kept in oven to be dry at 100 °C for 30 minutes. In that way, C-TiO₂ CE were fabricated and ready to be used in the DSSC.

3.1.3 Fabrication of Photoanode

To fabricate the working electrode, the titania nanoparticle slurry/paste was prepared as reported in another study[13], 2g of TiO₂ containing 15ml ethanol, 1ml distilled water and a drop of nitric acid solution, was stirred for 5hr by using magnetic stirrer(VELP Scientifica) to make homogenous paste/slurry. The prepared paste/slurry was deposited onto the fluorine doped tin oxide (FTO) glass substrate by employing the doctor blade coating method. After that, slurry on FTO was allowed to dry and annealed at 450°C for 1hr to eliminate impurities such as residual organic and moisture, that comes from the ambient air. After annealing, samples were allowed to cool, and then immediately immersed into an ethanol solution of 0.5mM N-719 dye molecules for 24 hours. After getting samples out of the dye solution, the titania samples adsorbed with dye were washed.

3.1.4 Fabrication of DSSC's

To fabricate the DSSC, CEs with different weigh ratios of carbon and photoanodes were prepared as explained above. In DSSC fabrication process, the CE, photoanode, spacer and electrolyte were used. To combine both CE and photoanode material, a spacer of 25µm was used, spacer was kept on the photoanode and heated it to make bond. Subsequently, photoanode and CE were clipped together through the clipper pins. Electrolyte solution containing 500mM 4-tert-butylpyridine, 100mM tetraethylammonium iodide, 100mM tetrabutylammonium iodide, 100mM LiI, 100mM KI and 50ml acetonitrile, was injected into the gap formed by the electrodes by capillary action. The DSSC's were tested under the 1.5 air mass (AM), 100mWcm⁻² stimulated light conditions to check the efficacy of the fabricated dye-sensitized solar cells.

3.1.5 Characterization of CEs

X-ray diffractograms of the fabricated CEs and pristine titania were obtained using X-ray Diffraction technique (XRD, D8 Advance Bruker Advanced, Germany) having a monochromatized radiation source of Cu-K α ($\lambda = 1.5418 \text{ \AA}$). All the samples were scanned to plot the data with a 2θ range of 10°–70° with a step rate of 0.02/sec. To analyze the surface morphology and the elemental composition of the C-TiO₂ powder films on

FTO, SEM/EDS analysis was carried out on an SEM/EDS analyzer having 20 kV accelerating voltage (Model JSM-6490A of JEOL, Japan) along with an X-ray energy dispersive spectrometer (EDS) analyzer. Samples were coated with gold in a vacuum sputter coater before SEM/EDS analysis. Raman spectra of the C-TiO₂ powder samples were obtained at room conditions by using Raman spectrometer (Model BTC162E-532S-SYS, BWTEK, USA) to collect the data between the 300 to 2100 (cm⁻¹) Raman shift range with the 532 nm laser excitation, to identify the carbon and titania peaks. To know the electrocatalytic activity of the CEs, cyclic voltammetry was performed by using the electrochemical workstation (Model 660E, CH Instruments, USA). In the three-electrode assembly, the working electrodes were used as a proposed CE, the Pt wire was used as a CE, while the reference CE was Ag/AgCl. All the CV measurements were performed in the acetonitrile solution containing 500mM LiClO₄, 10mM I₂ and 50mM LiI to be used as an electrolyte. J-V curves were by using a solar simulator with 100 mW cm⁻² simulated light power under 1.5 AM conditions.

3.2 Review of Synthesis Methods

Structural and morphological properties of CEs are dependent upon the synthesis methods. Their particle size, porosity, surface area, conductivity, electrocatalytic activity, reduction of triiodide ions, all the parameters are associated to the concerned preparation technique. Highly catalytic active CE material possess the large surface area and the small particle size. Here are the four important synthesis methods for CE,

- Thermal decomposition
- Hydrothermal Method
- Chemical vapor deposition

3.2.1 Thermal Decomposition

In the thermal decomposition method, heat is provided to the material which is intended to break into its components or to break its chemical bond, to get the required product. To synthesize a porous structure based CE, thermal decomposition method is used, that is an endothermic process in nature. In a study reported in 2012, Lan used this method to synthesize Pt CE[1].

3.2.2 Hydrothermal Method

Hydrothermal is most favorable and usually used to prepare CEs for DSSCs. It is used for producing fine crystals of the substances. In a study published by Morey and Niggli, explained this process in which the elements are under at high temperature and pressure in the presence of solvent (aqueous or non-aqueous)[2]. First of all precursors are properly mixed with each other via magnetic stirrer or manual stirring, then it is kept in the autoclave vessel at high temperature and pressure. The vessel used inside the autoclave is made up of Teflon material and have high tolerance towards extreme conditions. The operating parameters and reactions path matters a lot to produce controlled growth of shape, grains and their sizes. It is a methods that is usually used, cost effective technology and environmental friendly method of producing CEs. Figure 3-3 shows the diagram of the hydrothermal synthesis method.

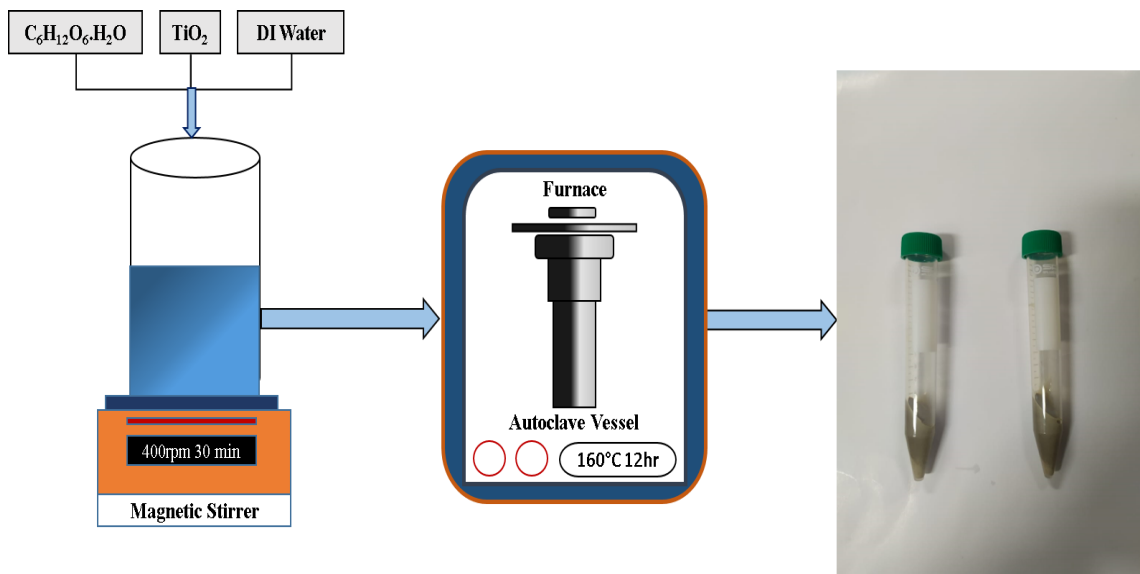


Figure 3-1 Schematic diagram of hydrothermal synthesis method

3.2.3 Chemical vapor deposition

Chemical vapor deposition (CVD) is a process in which through a controlled way, a solid material is vaporized and epitaxial grow on the surface of a substrate. It is also called deposition of thin films, and used for various applications such as in electronics, catalysis, CE for cells and other semiconductor related applications.

It is a sophisticated and versatile way to grow thin films with controlled thickness, size, porosity and other related parameters on the surface of substrate. This cost effective method employed for the 2-D materials like carbon, graphene, oxides, and transition metals to get highly ordered, highly pure and homogeneous thin films. Operating conditions plays an important role and morphology and compositions of the materials depends upon the chosen precursors and the type of substrate. Atomic layer deposition (ADL) is a prime example of CVD, which is a self-limiting reaction technique of precursors. Figure 3-4 clearly shows the CVD of graphene on the substrate[3].

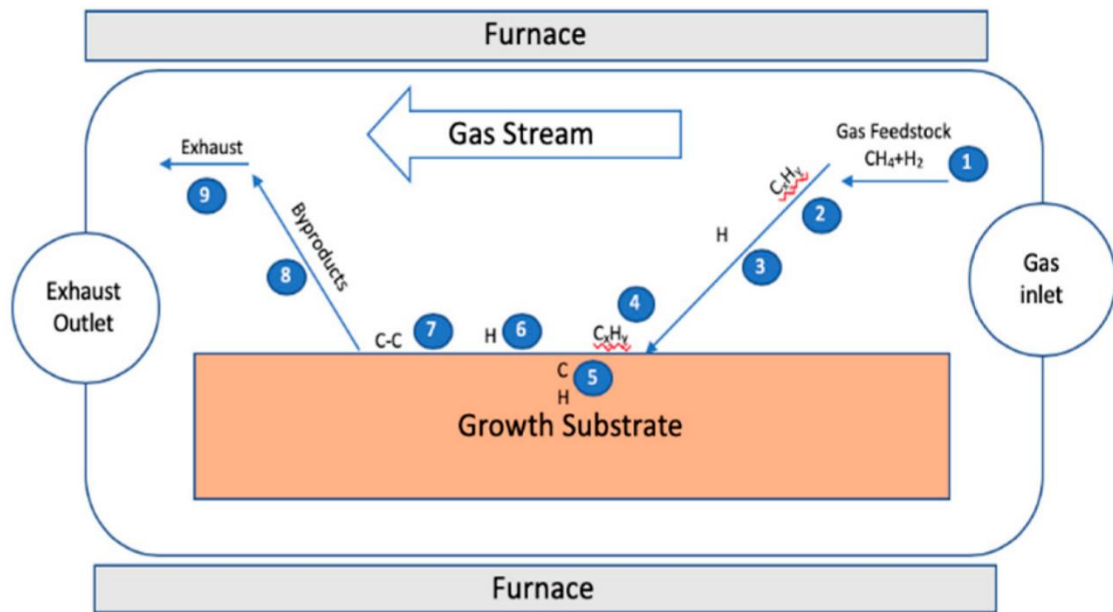


Figure 3-2 Chemical vapor deposition of graphene on the surface of substrate

3.3 Review Techniques of Fabrication of DSSC

When material is synthesized with appropriate technique, then it is fabricated onto the conductive substrates through various coating techniques that are mentioned below.

3.3.1 Doctor blade

Doctor blade coating also called knife coating, is a versatile and cost effective method of growing thin films on the substrates. First of all a paste containing material is formed by mixing the precursors in the liquid based solution such as volatile substance, and then paste through the blade onto the surface of the substrate. All the sides of the substrate FTO or TCO are tapes and only area where films is being deposit should be exposed. Manually,

film deposited in one go, and the gap between the blade or knife and the substrate surface basically defines the thickness of the thin films, the conductive and catalytic properties highly depend upon the thickness. The thickness of thin films ranging from 10-150 μm respectively, in this coating method[4]. After forming the films, the substrates are kept in the dry oven, so that volatile liquid substance may evaporate and pure thin films are ready for further characterization processes.

3.3.2 Spin coating

Spin coating is a more sophisticated and systematic way of growing thin films on the conductive glass slides. This method is more precise and controllable as well as thickness of the films is in nanometers, while in doctor blade it ranges in micrometers[5].

The process of spin coating completes in four stages,

- Deposition
- Spin up.
- Spin off
- Evaporation

In this process, solution of the material and the volatile solvent are spun at high speed, and then due to the centripetal force and surface tension of the liquid molecules, it makes covering on substrate. Sometimes solution is casted onto the substrate already, then it spreads over the films due to the centrifugal force, otherwise substrate keeps moving and material is dropped onto the substrate. After depositing the films, it is spin off and the substrate with thin films are kept in the oven to dry the films or to evaporate the volatile substance. Its main advantage over other techniques is to get required thickness films with



Figure 3-3 Modern spin coater for sophisticated coating

uniformity for better response. In short, it is widely used technique and is being used not only in R&D purposes, while using in industrial processes as well for better performance. Figure 3-5 shows the modern SEM instrument.

3.3.3 Screen printing

Screen printing is a technique used for coating films onto the FTO glass in a cost-effective manner[6]. Cobalt sulphide films was created by screen printing a conducting substrate and achieving 7.2 % PCE.

3.4 Review on Characterization Techniques

After synthesizing and fabrication of CE material, the CE material is characterize through various techniques such as XRD, SEM, EDS, and Raman Spectroscopy and with others as well. All of the techniques are discussed below in detail.

3.4.1 X-ray diffraction

X-ray diffraction is a material characterizing technique that identify the phase identification and structural information of the crystalline materials[7]. The material is finely grinded to make it powder, as well as thin films on the conductive glass substrates can also be examined.

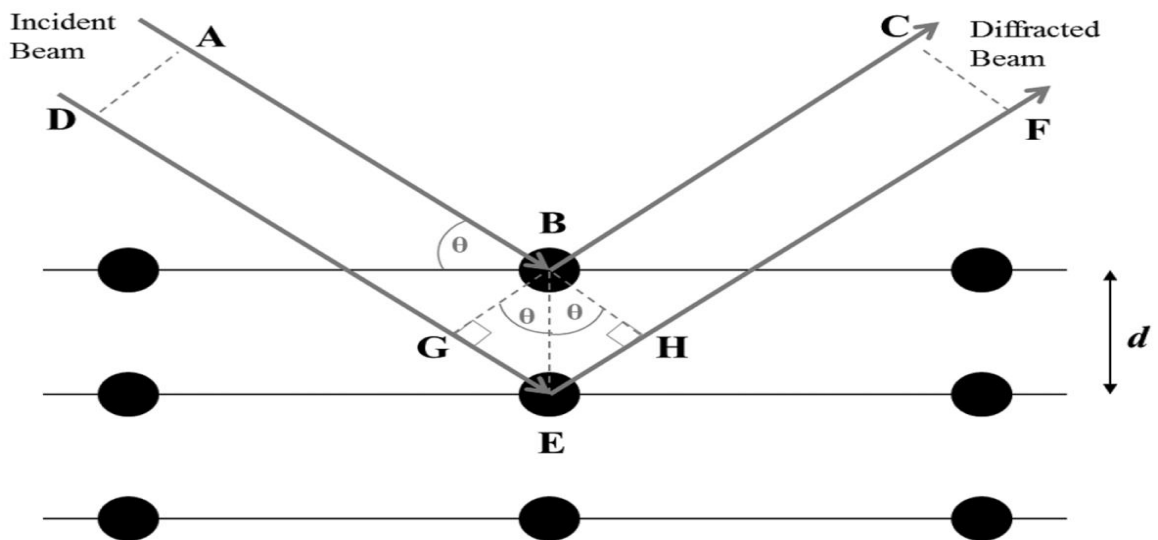


Figure 3-4 Interaction of the x-ray electromagnetic radiations with the crystalline material in XRD

3.4.1.1 Working principle

The process of X-ray diffraction is based on the constructive interference of monochromatic X-rays and a crystalline sample. A cathode ray tube generates these X-rays, which are then filtered to produce monochromatic radiation, collimated to concentrate, and directed toward the sample. When the incident rays interact with the sample, they produce constructive interference (and a diffracted ray) if the conditions fulfill Bragg's Law ($n\lambda=2d \sin\theta$). This law describes the relationship between the wavelength of electromagnetic radiation and the diffraction angle and lattice spacing in a crystalline sample. Figure 3-6 clearly shows the interaction of the x-ray electromagnetic radiations with the crystalline material that molecules are orderly arranged.

3.4.2 Scanning electron microscope

Scanning electron microscope also called FESEM is used to see the morphology, topography and structure of the coated thin films. SEM magnifies up to 300,000X and has an effective length ranging from 1 μ m to 10nm.

3.4.2.1 Working principle

Under vacuum, a primary electron beam is generated and scanned across the surface. When an electron is struck by a specimen, a secondary electron beam and back scattered electrons are produced, resulting in variations in signals that provide an image of the surface.

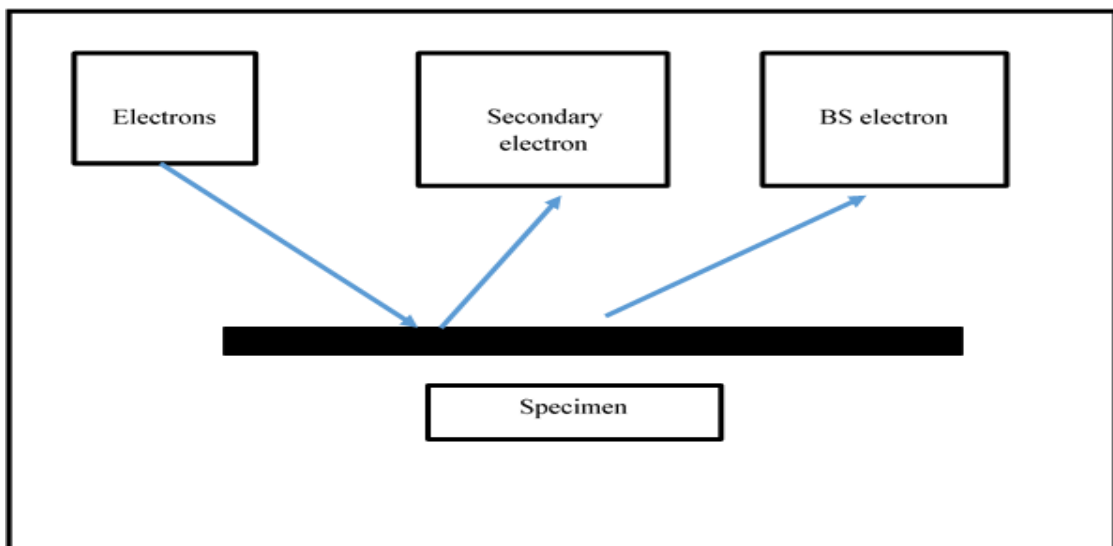


Figure 3-5 Probe beam and measuring particle in SEM

Electrons released from a heated filament that are accelerated toward the sample. The electrons interact with the sample atoms, resulting in secondary electrons, characteristic X-rays, and electrons dispersed backwards. The first electromagnetic lens de-magnifies the primary beam of the second electromagnetic lens. These signals are identified by a detector. Backscattered electrons are produced as a result of elastic distribution. Along with the cathode ray tube, the detector generates the micrograph image. Electron beam interaction with the specimen is shown in Figure 3-7.

3.4.2.2 Sample preparation

Sample preparation is a critical step in SEM imaging. If the sample is in powder form, it is simply placed on a stub, coated with a conductor if an insulator is used, and an image is obtained. Substrates are properly prepared if films are being examined. Figure 3-8 depicts the preparation steps.

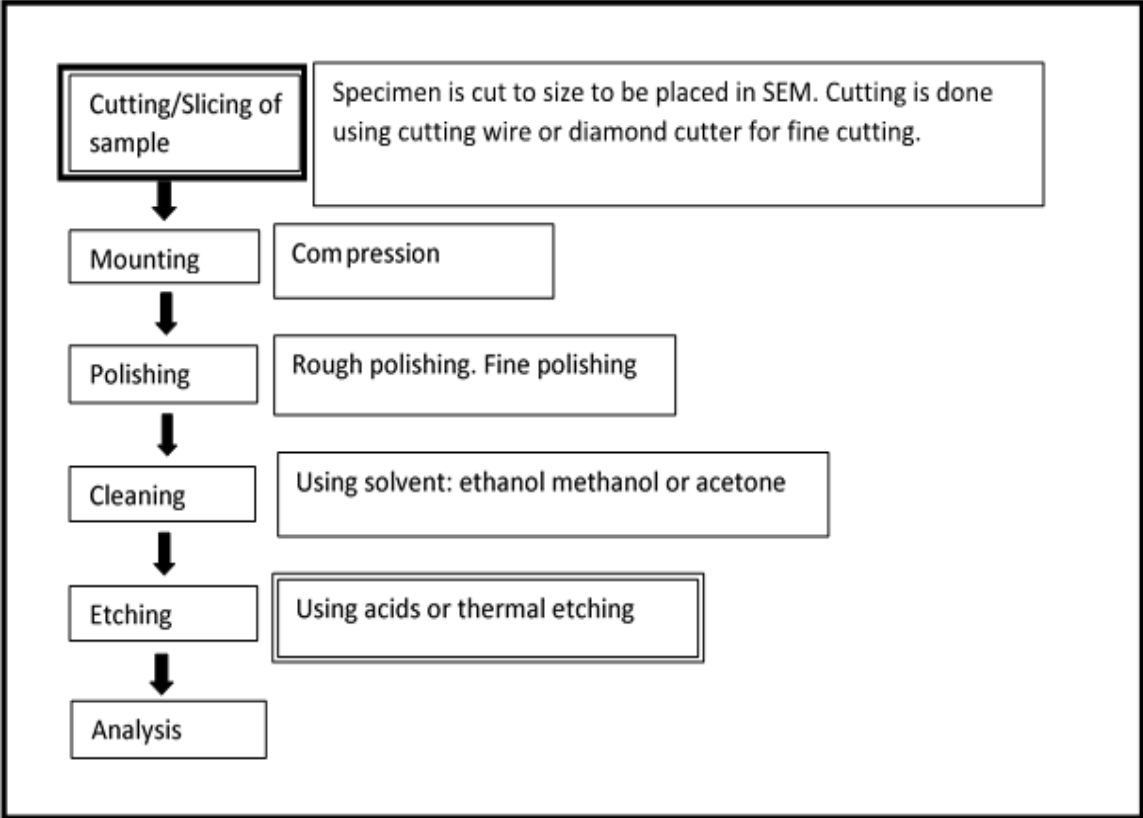


Figure 3-6 Schematic flow for sample preparation for SEM films

3.4.3 Energy dispersive X-ray Spectroscopy

EDS or EDX is a compositional elemental analysis technique used to characterize a specimen's chemical composition. The EDS pattern is the result of X-ray absorption by semiconductors; this absorbance excites the crystal electrons, which move to the

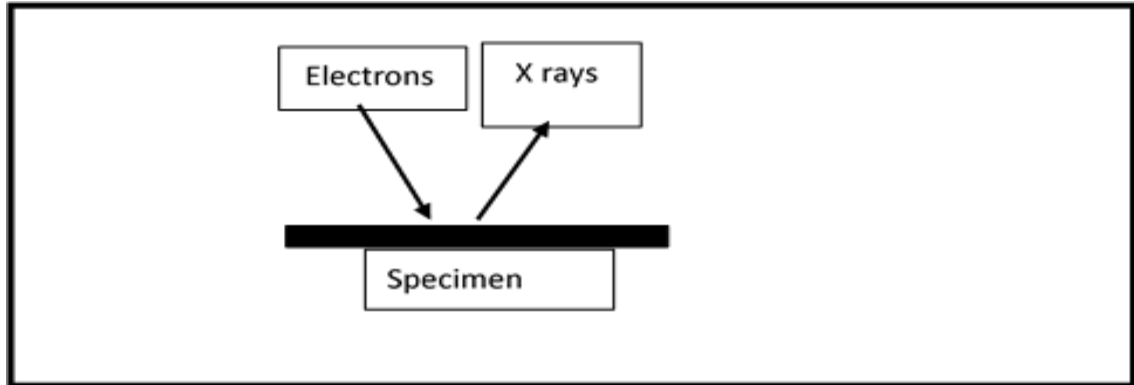


Figure 3-7 Electron interaction with specimen during EDS

conduction band, resulting in an electric pulse that corresponds to the energy of X-beams that are included and coordinated in a multichannel analyzer, and an introduction of sign solidarity against its energy gives the required range. Figure 3-9 shows the electron interaction with specimen during EDS.

When electrons interact with the sample, the electrons gets excited and leave empty spaces. These vacancies are filled by electrons in higher shells. Energy is released in the form of X-rays and all elements emit X-rays with distinct energy levels. Each element in the periodic table has a unique energy value, which allows for elemental analysis using EDS.

The letters K, L, M represent the shells from which electrons are emitted, and the letters,, represent the shells from which they are substituted. The sample is prepared in the same way as for SEM. In theory, EDS can detect all elements in the periodic table from beryllium to uranium.

3.4.4 Raman Spectroscopy

Raman spectroscopy is an analytical technique that uses scattered light to measure a sample's vibrational energy modes[8]. It is named after the Indian physicist C. V. Raman, who discovered Raman scattering in 1928 with his research partner K. S. Krishnan.

3.4.4.1 Principle of Raman Spectroscopy

Raman spectroscopy is based on Raman scattering (or the Raman Effect), which reveals molecules' vibrational, rotational, and other low frequency modes. The sample is exposed to an intense beam of monochromatic light (typically a laser beam) in the visible, near-infrared, or near-ultraviolet frequency range. Electromagnetic radiation can be transmitted, absorbed, or scattered when it interacts with a substance. When the sample molecules are scattered by monochromatic radiations, then majority of the radiation

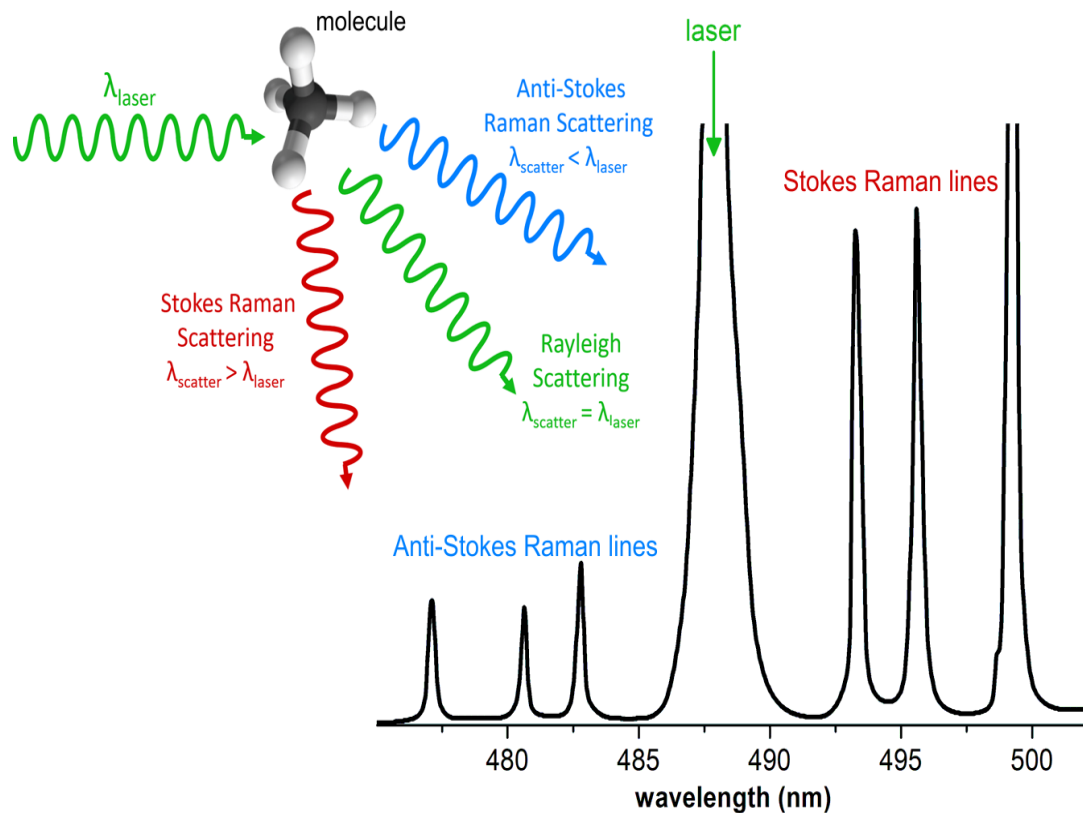


Figure 3-8 Laser interaction with the specimen and Raman spectrum with intensity peaks undergoes common Rayleigh scattering (the frequency/wavelength of the radiation remains unchanged). However, a small percentage of the scattered radiation has a slightly different frequency than the incident radiation. This is referred to as the Raman Effect[9]. The frequency shifts are nearly independent of the excitation wavelength and are unique to the substance/molecule. Raman spectra and laser interaction with the sample can be clearly shown in Figure 3-10[10].

3.4.5 Cyclic Voltammetry

Cyclic voltammetry is an electrochemical technique used to measure the current response of a redox active solution to a linearly cycled potential sweep between two or more fixed values. It is a useful method for rapidly determining information about the thermodynamics of redox processes, the analyte's energy levels, and the kinetics of electronic-transfer reactions[11]. Like other voltammetry techniques, it is also a three electrode assembly which contains

- Working electrode (Usually glassy carbon is used)
- CE (Usually Pt wire is used)
- Reference electrode (Usually Ag/AgCl is used)

The prepared CE paste is formed by mixing the material with nafion that acts as a binder as well as absolute alcohol, though to test the electrocatalytic activity of CE, but it always be coated onto the working electrode that is basically glassy carbon. All these electrodes are dipped into the electrolyte solution and make proper contact with the system through probes, after that voltage window range and other related parameters are selected to get the spectra of cyclic voltammetry of a given coated material onto the working electrode.

Summary

In the chapter 3 synthesizing, fabrication and characterization have been discussed related to the CE material for the DSSC applications. In synthesizing techniques, the different methods and different processes are adopted to make the CE material with their advantages and disadvantages and which technique is more preferred over others. In fabrication process, different coating methods are being used to coat the sample paste with the volatile solvent over the surface of the substrates to form thin films with controlled thickness. Last but not least, after fabricating the CE material, the prepared samples of CE were characterized through various techniques from material structure identification, material morphology to electrocatalytic activity to know the material property and behave towards the solar cell applications.

This chapter also briefly discussed the synthesis of the C-TiO₂ CEs for DSSCs. Titania and glucose monohydrate precursors have been used for the preparation of CE, because of their good conductive and electrocatalytic properties. Carbonaceous materials have been shown good performance as CE. Titania is nontoxic, abundantly available and environmental friendly material. To use both of them together, to get high conductive and electrocatalytic composite material, and it exhibits good properties and showed comparable photo conversion efficiency. After that to make the DSSC, the fabrication of photoanode containing TiO₂ with dye molecules have been fabricated, and in the final step the DSSC solar cell is formed by clipping photoanode and CE together with electrolyte solution between them.

References

- [1] Z. Lan, J. Wu, J. Lin, and M. Huang, “Morphology controllable fabrication of Pt CEs for highly efficient dye-sensitized solar cells,” *J. Mater. Chem.*, vol. 22, no. 9, pp. 3948–3954, Feb. 2012.
- [2] G. W. Morey and P. Niggli, “The Hydrothermal Formation of Silicates, A Review,” *J. Am. Chem. Soc.*, vol. 35, no. 9, pp. 1086–1130, Sep. 2003.
- [3] M. Saeed, Y. Alshammari, S. A. Majeed, and E. Al-Nasrallah, “molecules Chemical Vapour Deposition of Graphene-Synthesis, Characterisation, and Applications: A Review.”
- [4] “Sol-Gel Technologies for Glass Producers and Users - Google Books.”
- [5] M. Pichumani, P. Bagheri, K. M. Poduska, W. González-Viñas, and A. Yethiraj, “Dynamics, crystallization and structures in colloid spin coating,” *Soft Matter*, vol. 9, no. 12, pp. 3220–3229, Mar. 2013.
- [6] S. Ahmadi, N. Asim, M. Alghoul, ... F. H.-I. J. of, and undefined 2014, “The role of physical techniques on the preparation of photoanodes for dye sensitized solar cells,” *hindawi.com*.
- [7] “X-ray Powder Diffraction (XRD).” [Online]. Available: https://serc.carleton.edu/research_education/geochemsheets/techniques/XRD.html. [Accessed: 13-Feb-2022].
- [8] C. V. Raman and K. S. Krishnan, “A New Type of Secondary Radiation,” *Nat. 1928 1213048*, vol. 121, no. 3048, pp. 501–502, 1928.
- [9] “Principles of Raman spectroscopy (1) What is Raman spectroscopy? | JASCO Global.” [Online]. Available: <https://www.jasco-global.com/principle/1-what-is-raman-spectroscopy/>. [Accessed: 14-Feb-2022].
- [10] “3.2. Raman spectroscopy.” [Online]. Available: <https://sisu.ut.ee/heritage-analysis/book/export/html/19022>. [Accessed: 14-Feb-2022].
- [11] “Cyclic Voltammetry Basics, Setup & Applications | Ossila.” [Online]. Available:

<https://www.ossila.com/pages/cyclic-voltammetry>. [Accessed: 14-Feb-2022].

- [12] G. Huang, C. H. Lu, and H. H. Yang, “Magnetic Nanomaterials for Magnetic Bioanalysis,” in *Novel Nanomaterials for Biomedical, Environmental and Energy Applications*, Elsevier, 2018, pp. 89–109.
- [13] K. Wang, R. Ding, Y. Cui, and K. Hong, “A simple method to synthesize low-cost carbon modified TiO₂ CEs for high-efficiency dye-sensitized solar cells,” *Mater. Res. Express*, vol. 6, no. 8, Jun. 2019.

Chapter 4: Results and Discussion

4.1 Results and Discussion

4.1.1 X-Ray Diffraction

X-ray diffraction patterns of pristine anatase titania and C-TiO₂ powders are given in Figure 4-1. As it is clear, the pristine anatase titania phase (PDF#12-1272) major peak are present at $2\theta=25.3^\circ$ and 48.1° , which corresponds to the (101) and (200) planes of anatase titania respectively[1]. From the different C-TiO₂ powders diffractograms, it is quite evident that carbon doping into the titania is responsible for the distortion of anatase titania tetragonal structure, as Ti-C has a longer bond length than-O, and carbon has a higher

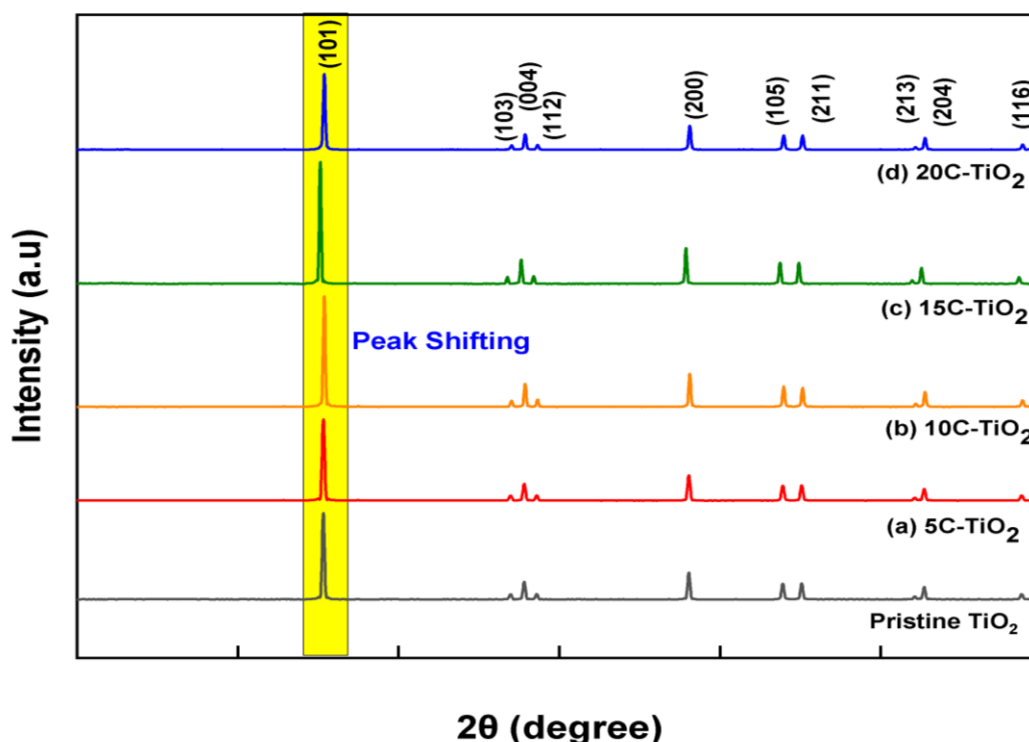


Figure 4-1 XRD patterns of pristine TiO₂ and C-TiO₂ powders respectively atomic radius than oxygen[2] and no diffraction peak of carbon observed in the xrd pattern because carbon is present in an amorphous phase.

It is clearly shown in the graph by increasing doping of the carbon in anatase titania powder, the peak intensities at (101) and (200) of the C-TiO₂ powder samples increases respectively, that showed the crystallinity of the samples had been increased as well[3].

The grain size of the C-TiO₂ powder samples found out by using the scherrer equation as shown in Eq(1)[4].

$$L = \frac{k\lambda}{B\cos\theta} \quad \text{Eq(1)}$$

Where k is the scherrer constan, λ represents the wavelength of the X-ray source(which is 1.5403Å), B is FWHM of the diffraction peak at angle 2Θ , and L indicates the size of the sample, while Θ is the Bragg angle.

The grain size of the pristine titania was calculated 54.4 nm, while the most crystalline powder material appeared to be 15C-TiO₂ as it depicts the highest peak intensity, showed the better crystallite size 55.5nm. Overall this increment in peak intensities and slightly peak shifting shows the inclusion of carbon in anatase titania phase. As 20C-TiO₂ powder material showed a weak intensity peak in comparison to other C-TiO₂ powders materials, due to the poor interconnection and less adherence between anatase titania and carbon[5][6].

4.1.2 SEM/EDS

The morphology and composition of the CEs are key elements that strongly affect the overall efficiency of the DSSC. The morphological images and the EDS spectra of the C-TiO₂ films were analyzed by using SEM. For better redox reactions or the better reduction of triiodide ions(I₃⁻), the C-TiO₂ films structure should be porous[1], [7].Figure 4-2 shows the morphology and EDS spectra of 5% C-TiO₂ (a,a1,a2), 10% C-TiO₂ (b,b1,b2),15% C-TiO₂ (c,c1,c2) and 20% C-TiO₂(d,d1,d2) calcined at 500°C with low (10µm) and high (1µm) magnifications respectively. Doctor blade coating was used to coat C-TiO₂ paste onto the FTO. C-TiO₂ powder morphological images appear to be a mix of spherical and elliptical nanoparticles randomly distributed with porous structure at 10µm and 1µm respectively. As the CEs porous structure doesn't show only high surface area (active sites present) but active participation in the redox reactions, especially in the reduction of triiodide ions(I₃⁻) that present in the electrolyte[7][8], responsible for the overall efficiency of the DSSC.

EDX spectra of the CEs show the elemental composition of the carbon, titanium, and oxygen weight percentages as shown in Figure 4-2 (a2, b2, c2, d2) respectively. Carbon

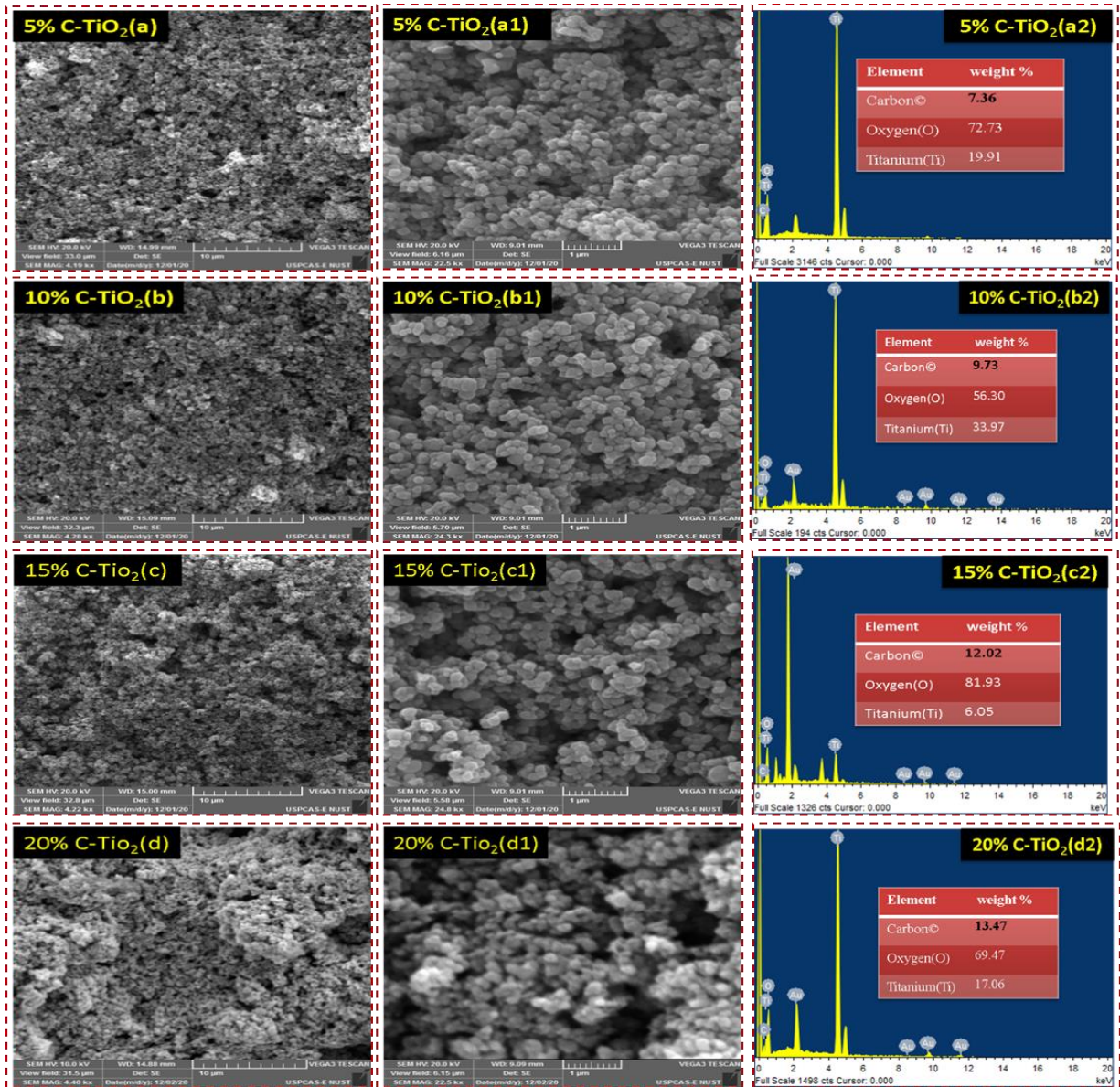


Figure 4-2 SEM images and EDS spectra of a,a1,a2) 5% C-TiO₂, b,b1,b2) 10% C-TiO₂, c,c1c2) 15% C-TiO₂ and d,d1,d2)20% C-TiO₂ at 10 μ m and 1 μ m respectively

weight percentage increases, as doping concentration increased in titania 7.36%,9.73%,12.02% and 13.47% for 5% C-TiO₂ , 10% C-TiO₂,15% C-TiO₂ and 20% C-TiO₂ respectively. Carbon peaks present in the EDX spectra confirm the anchoring of carbon nanoparticles on the TiO₂.

4.1.3 Raman Spectroscopy

Figure 4-3 shows the Raman spectra of C-TiO₂ powder samples, a) 5C-TiO₂ b) 10C-TiO₂ c) 15C-TiO₂ and d) 20C-TiO₂ respectively. Two peaks present at 1359 cm⁻¹ (D-band) and 1593 cm⁻¹ (G-band) confirm the presence of porous carbon spheres[9], G-band peak intensity is greater than D-band, shows the increasing degree of graphitization of

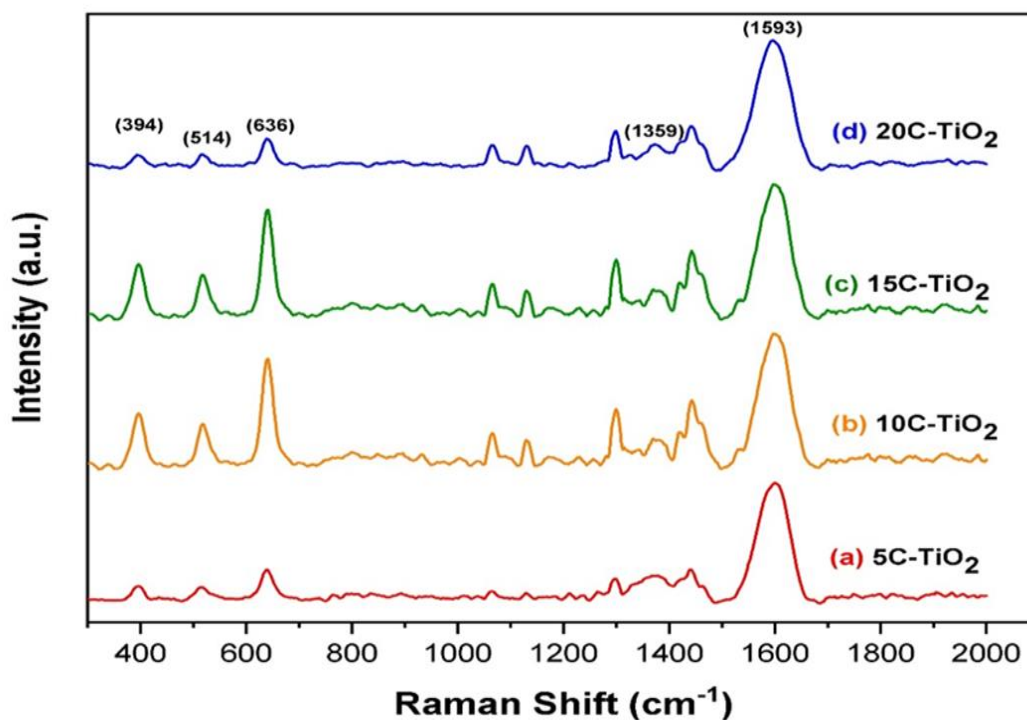


Figure 4-3 Raman Spectroscopy of carbon doped titania CEs a) 5C-TiO₂, b) 10C-TiO₂, c) 15C-TiO₂, and d) 20C-TiO₂ respectively

carbon[10], and three other weak peaks present at 394 cm⁻¹, 514 cm⁻¹, and 636 cm⁻¹ which corresponds to the anatase titania peaks[1][11]. Raman results are consistent with XRD results as crystallinity increases first and then decreases with more percentage of C-TiO₂ powder samples.

4.1.4 Cyclic Voltammetry

To know the electrocatalytic activity of the C-TiO₂ CEs, cyclic voltammetry was performed. To make the slurry of the C-TiO₂ powders, ink was prepared in the 10 ml glass vial containing 80 ul ethanol, 2 ul of nafion as a binder and 2 mg of each of the C-TiO₂ material powder, sonicate the solution for 2 hours to make sure the proper homogeneous mixture, then 05 ul of the ink deposited on the disk electrode through the micro pipette and

dried it. The voltammograms of the C-TiO₂ CEs (5C-TiO₂, 10C-TiO₂, 15C-TiO₂, 20C-TiO₂) and platinum (Pt) CE are clearly shown in Figure 4-4. Redox peaks of all the CEs

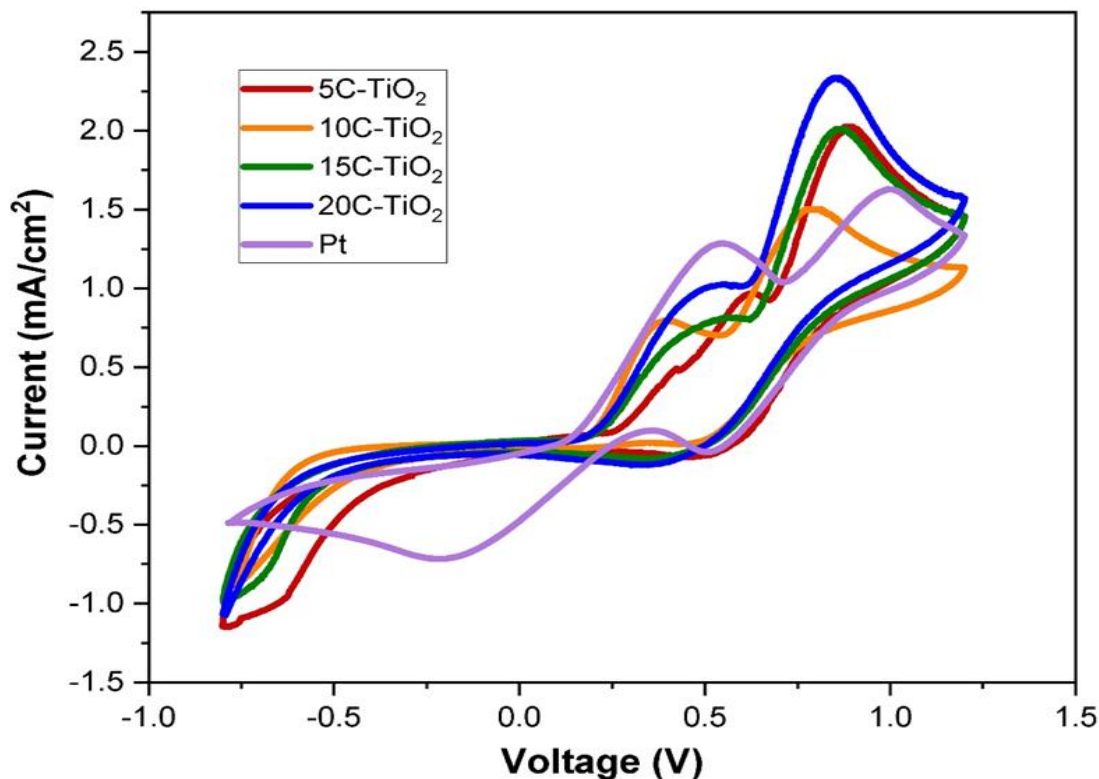


Figure 4-4 Cyclic voltammograms obtained at scan rate of 100mV/sec for C-TiO₂ CEs and platinum respectively, in an electrolyte containing 500mM LiClO₄, 10mM I₂ and 50mM LiI in acetonitrile solution

were observed between the voltage window ranging from -0.8V to 1.2V at the scan rate of 100mV/sec, in an electrolyte containing 500mM LiClO₄, 10mM I₂, and 50mM LiI in the acetonitrile solution[12]. The upward or positive side and downward peaks or negative side of the CEs are showing the anodic peaks (oxidation) and cathodic peaks (reduction) respectively[13]. The anodic peaks in the CV curve relates to the oxidation of iodide and triiodide ions, while cathodic peaks correspond to the reduction of triiodide ions, these phenomenons have shown by the Eq (2) and Eq (3) respectively[14].

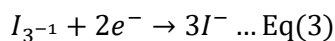
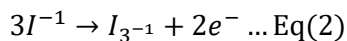


Figure 4-4 showing the voltammograms of the C-TiO₂ and Pt CEs, the redox peaks of all the C-TiO₂ CEs are in phase with the Pt, which means they are following the same

electrocatalytic activity pattern as of the Pt. In the oxidation peak it is clearly shown the c-TiO₂ have higher current density as compared to Pt CE. Hence it showed that, the C-TiO₂ CEs are able to transport the charge actively and have good activity towards the redox couple, as they are in correspondence with the Pt characteristics. In DSSCs, CEs is responsible for the reduction of the triiodide ion, allowing the dye molecules to regenerate for the photo generation phenomenon, fast charge transfer, and low recombination rate in the redox mediator and oxidized dye molecules.

4.1.5 I-V Characteristic Curve

The photocurrent density-voltage (J-V) curves of the DSSC's were performed to assess the efficacy of the DSSCs solar cells, by using identical photoanodes and carbon-doped titania (5C-TiO₂, 10C-TiO₂, 15C-TiO₂, 20C-TiO₂) and Pt CEs are shown in Figure 4-5 and their summary of photovoltaic parameters containing open-circuit voltage V_{oc} (V), short circuit current density J_{sc} (mA cm⁻²), fill factor FF (%) and efficiency η (%) are given in Table4.1. The efficiencies and fill factors of the solar cells have been calculated by using the formulas given in Eq(4) and Eq(5)[15].

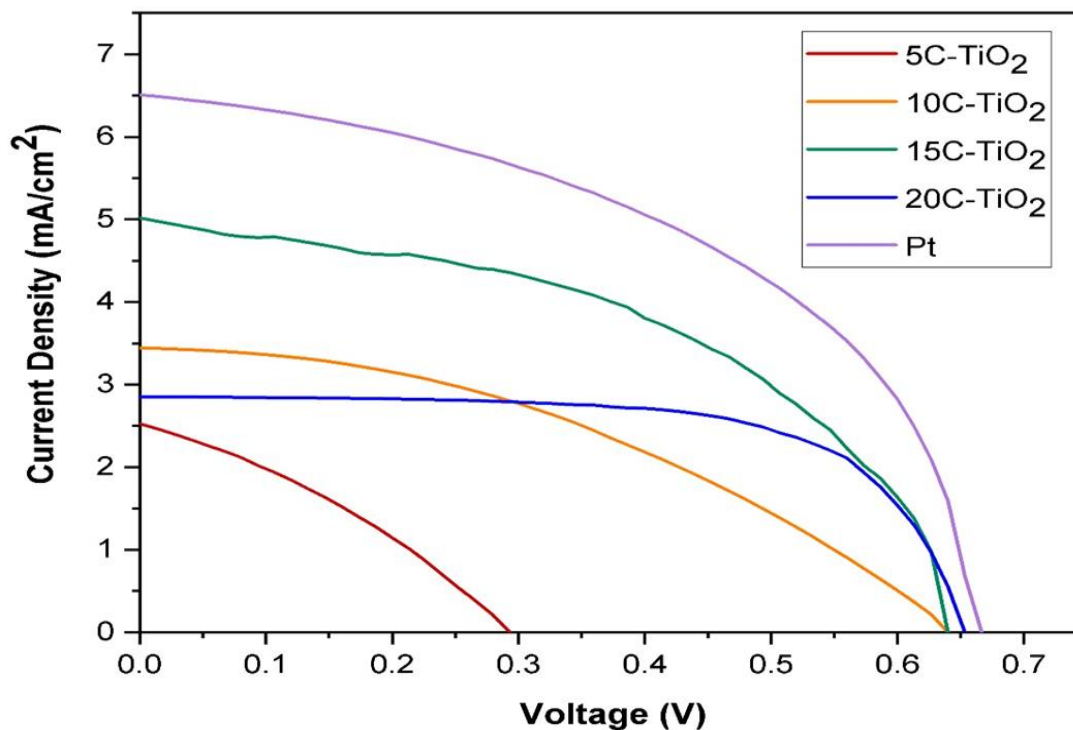


Figure 4-5 Photocurrent density-voltage characteristics curves of C-TiO₂ and Pt CEs

$$\eta (\%) = \frac{V_{\max} * J_{\max} * 100 \%}{P_{in}} \quad \dots \text{Eq(4)}$$

$$FF = \frac{V_{\max} * J_{\max}}{V_{oc} * J_{sc}} \quad \dots \text{Eq(5)}$$

The reference DSSC with Pt CE has 2.12% efficiency, while other DSSCs solar cells using carbon-doped titania 5C-TiO₂, 10C-TiO₂, 15C-TiO₂ and 20C-TiO₂ showed efficiencies 0.24%, 0.88%, 1.56% and 1.23% respectively.

As the loading of carbon concentration increases, the short circuit current density increases except for the 20C-TiO₂ CE, the same is the case with efficiency. Fill factor values of the CEs are also increased with the doping. Low carbon doping concentration into titania is responsible for the better adhesion between the FTO and the CEs, but leads to poor reduction of triiodide ions reduction due to the low surface area of the CEs, on the other hand, for the 20C-TiO₂ CE, it has enough surface area for the triiodide ions reduction, but adhesion is too weak between FTO and the C-TiO₂ CEs[5], that makes it less efficient at higher carbon dopings. So, the optimized DSSC with 15C-TiO₂ has higher efficiency as well as good adhesion and reduction properties as compared to other C-TiO₂ except for Pt. Pt has higher efficiency due to the super electrocatalytic active features.

Table 4-1 Photovoltaic properties of the DSSCs using C-TiO₂ and platinum as CEs

CEs	Photovoltaic Parameters of DSSC			
	V _{oc} (V)	J _{sc} (mA cm ⁻²)	FF (%)	η (%)
C-TiO₂ Materials				
5C-TiO ₂	0.29	2.52	32.8	0.24
10C-TiO ₂	0.64	3.44	39.8	0.88
15C-TiO ₂	0.64	5.01	48.4	1.56
20C-TiO ₂	0.65	2.85	65.8	1.23
Platinum	0.67	6.50	48.9	2.12

The best 15C-TiO₂ CE solar cell has 1.56% efficiency, which is more than 73.5% that of Pt-based CE solar cell that has 2.12% efficiency. Moreover, 15C-TiO₂ CE parameter values like, fill factor 48.4%, short circuit current density 5.01 mA cm⁻², and open-circuit voltage 0.64V are quite closer to Pt's fill factor 48.9%, short circuit current density mA cm⁻², and open-circuit voltage 0.67V respectively.

Summary

In this chapter the fabricated CEs were characterized by using various techniques through which DSSC were analyzed. First of all, the phase identification of the CEs were detected by XRD. The elemental composition and morphology of the fabricated CE thin films were checked through the SEM and EDS respectively. The presence of the titania and the porous carbon also support to find out the intensity peaks at specific wavelengths. To check the conductivity and electrochemical activity of the CE were tested through the cyclic voltammetry technique, that shows the oxidation and reduction peaks that are in comparison with the Pt CE. Among the different ratios of C-TiO₂ CEs, the CEs with 15% C-TiO₂ showed better photo conversion efficiencies that was checked through the IV simulator technique. All the parameters of the DSSCs containing I_{sc}, V_{oc}, FF, and efficiencies are given in the table, shows their respective values and comparison with the Pt CE.

References

- [1] K. Wang, R. Ding, Y. Cui, and K. Hong, “A simple method to synthesize low-cost carbon modified TiO₂ CEs for high-efficiency dye-sensitized solar cells,” *Mater. Res. Express*, vol. 6, no. 8, p. 085553, 2019.
- [2] L. Ji, Y. Zhang, S. Miao, M. Gong, and X. Liu, “In situ synthesis of carbon doped TiO₂ nanotubes with an enhanced photocatalytic performance under UV and visible light,” *Carbon N. Y.*, vol. 125, pp. 544–550, 2017.
- [3] S. J. Park, H. Kim, Y. J. Kim, and H. Lee, “Preparation of carbon-coated TiO₂ nanostructures for lithium-ion batteries,” *Electrochim. Acta*, vol. 56, no. 15, pp. 5355–5362, 2011.
- [4] N. Ahmed, M. A. Iqbal, Z. S. Khan, and A. A. Qayyum, “DC Magnetron-Sputtered Mo Thin Films with High Adhesion, Conductivity and Reflectance,” *J. Electron. Mater.*, vol. 49, no. 7, pp. 4221–4230, 2020.
- [5] J. Lim, S. Y. Ryu, J. Kim, and Y. Jun, “A study of TiO₂/carbon black composition as CE materials for dye-sensitized solar cells,” *Nanoscale Res. Lett.*, vol. 8, no. 1, pp. 1–5, 2013.
- [6] J. Zhang, Z. H. Huang, Y. Xu, and F. Y. Kang, “Carbon-coated TiO₂ composites for the photocatalytic degradation of low concentration benzene,” *Xinxing Tan Cailiao/New Carbon Mater.*, vol. 26, no. 1, pp. 63–70, 2011.
- [7] E. Ramasamy, W. J. Lee, D. Y. Lee, and J. S. Song, “Nanocarbon counterelectrode for dye sensitized solar cells,” *Appl. Phys. Lett.*, vol. 90, no. 17, pp. 17–20, 2007.
- [8] “Synergetic Effects of Hybrid Carbon Nanostructured CEs for Dye.pdf.”
- [9] X. Chen *et al.*, “Synthesis, growth mechanism, and electrochemical properties of hollow mesoporous carbon spheres with controlled diameter,” *J. Phys. Chem. C*, vol. 115, no. 36, pp. 17717–17724, 2011.
- [10] H. J. Peng, G. X. Hao, Z. H. Chu, Y. W. Lin, X. M. Lin, and Y. P. Cai, “Porous carbon with large surface area derived from a metal-organic framework as a

- lithium-ion battery anode material,” *RSC Adv.*, vol. 7, no. 54, pp. 34104–34109, 2017.
- [11] F. Hardcastle, “Raman Spectroscopy of Titania (TiO₂) Nanotubular Water-Splitting Catalysts,” *J. Ark. Acad. Sci.*, vol. 65, pp. 43–48, 2011.
- [12] S. Shakir *et al.*, “Electro-catalytic and structural studies of DNA templated gold wires on platinum/ITO as modified CE in dye sensitized solar cells,” *J. Mater. Sci. Mater. Electron.*, vol. 29, no. 6, pp. 4602–4611, 2018.
- [13] R. Kumar, S. S. Nemala, S. Mallick, and P. Bhargava, “Synthesis and characterization of carbon based CE for dye sensitized solar cells (DSSCs) using sugar free as a carbon material,” *Sol. Energy*, vol. 144, pp. 215–220, Mar. 2017.
- [14] R. Kumar and P. Bhargava, “Synthesis and characterization of carbon based CE for dye sensitized solar cells (DSSCs) using organic precursor 2-2’Bipyridine (Bpy) as a carbon material,” *J. Alloys Compd.*, vol. 748, pp. 905–910, Jun. 2018.
- [15] R. Kumar, V. Sahajwalla, and P. Bhargava, “Fabrication of a CE for dye-sensitized solar cells (DSSCs) using a carbon material produced with the organic ligand 2-methyl-8-hydroxyquinolinol (Mq),” *Nanoscale Adv.*, vol. 1, no. 8, pp. 3192–3199, 2019.

Chapter 5: Conclusions and Future Recommendations

5.1 Conclusion

We successfully fabricated the DSSCs, by using C-TiO₂ material as CEs with different weight ratios, through the hydrothermal synthesis method, followed by calcination in the tube furnace. C-TiO₂ CE has many positive attributes such as high electrocatalytic activity in the form of reduction of triiodide ions present in the redox mediator, fast charge transfer rate, low recombination rate, fast regeneration of the dye molecules, and has quite closer power conversion efficiency to Pt. The best-optimized CE 15C-TiO₂ ratio has 1.56% photovoltaic efficiency, which is quite closer to Pt 2.12% efficiency. Structural, optical, morphological, electrochemical, and photovoltaic studies were carried out to assess the performance and behavior of the CE materials.

It shows the low cost, catalytic active, Pt free, excellent power conversion C-TiO₂ CEs have high enough potential to replace the expensive conventional Pt CE and the ability to be adopted at the commercial level for power applications.

5.2 Future Recommendations

Being a cost effective, easy and environmental friendly DSSC have great potential to replace the conventional first generation silicon based solar cells. Right now, DSSC have achieved an efficiency of 14%, to achieve efficiency more than 14%, extraordinary measures are needed and the recommendation are outlined below.

- Carbonaceous materials with conducting polymer are promising alternative composite
- Doctor blade coating is frequently used, but it's not a systematic approach, for its fabrication a systematic approach should be used such as spin coating, screen printing and EPD coating methods
- To prepare metal based and polymer conducting CEs, hydrothermal/ in situ polymerizations methods should to be used

- Use of natural sensitizer is a cost effective approach, because ruthenium based sensitizers are quite expensive and make DSSC expensive technology.
- Multiple layers of composites of CE can further improve the electro catalytic properties of the DSSC
- Carbon allotropes more enhance the light harvesting to absorbs more light
- To develop and explore Pt free cost effective new CEs should be prioritized

Appendix A- Publication

Performance analysis of carbon-doped titania (C-TiO₂) counter electrode (CE) for dye sensitized solar cells (DSSCs)

Faisal Abbas¹, Mustafa Anwar¹, Asif Hussain Khoja¹, Nadia Shahzad¹, Muhammad Tahir¹, Muniba Ayub¹, Sehar Shakir^{1*}

¹U.S.-Pakistan Centre for Advanced Studies in Energy (USPCAS-E), National University of Sciences & Technology (NUST), Sector H-12 Islamabad (44000), Pakistan

**Corresponding Author's Email: sehar@uspcase.nust.edu.pk*

Abstract

Platinum (Pt) is a super catalytic active metal that has long been used as a counter electrode (CE) in the dye sensitized solar cell (DSSC) applications, but its high-cost is a challenging factor for its commercial availability. In this study, we fabricated an efficient and low-cost carbon-doped titania (C-TiO₂) CE to replace Pt in DSSCs. By varying different weight ratios, C-TiO₂ were synthesized through the hydrothermal synthesis method followed by calcination in the tube furnace. Doctor blade coating method was used to deposit thin films on fluorine-doped tin oxide (FTO) substrates. Structural and morphological properties were studied by using various analytical techniques. Moreover, the electrochemical and photo conversion characteristics of the fabricated CEs were investigated to analyze their performance. Cyclic voltammetry (CV) results of the fabricated CEs showed the comparable electrocatalytic activity towards the reduction of the triiodide ions in the redox mediator as of Pt in the DSSCs. Meanwhile, photovoltaic measurements results showed the best performing 15% C-TiO₂ CE having 1.56% photoconversion efficiency (PCE) as compared to Pt that is 2.12%. This study proposed a simple method to fabricate an efficient and low-cost C-TiO₂ CE for DSSCs.
